Redox Biology 48 (2021) 102188

Contents lists available at ScienceDirect

Redox Biology

journal homepage: www.elsevier.com/locate/redox

Missense mutation in selenocysteine synthase causes cardio-respiratory failure and perinatal death in mice which can be compensated by selenium-independent GPX4

Noelia Fradejas-Villar [a], Wenchao Zhao [a,#], Uschi Reuter [a], Michael Doengi [b], Irina Ingold [c,1], Simon Bohleber [a], Marcus Conrad [c,d], Ulrich Schweizer [a,*]

[a] Institut für Biochemie und Molekularbiologie, Universitätsklinikum Bonn, Bonn, Germany
[b] Institut für Physiologie, Universitätsklinikum Bonn, Bonn, Germany
[c] Helmholtz Zentrum München, Institute of Metabolism and Cell Death, 85764, Neuherberg, Germany
[d] Pirogov Russian National Research Medical University, Laboratory of Experimental Oncology, Moscow, 117997, Russia

ARTICLE INFO

Keywords:
GPX4
Sedaghatian disease
Selenoprotein
NRF2
SEPSECS

ABSTRACT

Selenoproteins are a small family of proteins containing the trace element selenium in form of the rare amino acid selenocysteine (Sec), which is decoded by the UGA codon. In humans, a number of pathogenic variants in genes encoding distinct selenoproteins or selenoprotein biosynthesis factors have been identified. Pathogenic variants in selenocysteine synthase (SEPSECS), which catalyzes the last step in Sec-tRNA$^{[Ser]Sec}$ biosynthesis, were reported in children suffering from progressive cerebello-cerebral atrophy. To understand the pathomechanism associated with *SEPSECS* deficiency, we generated a novel mouse model recapitulating the respective human pathogenic p.Y334C variant in the murine *Sepsecs* gene (*Sepsecs*^{Y334C}). Unlike in patients, pups homozygous for the p.Y334C variant died perinatally with signs of cardio-respiratory failure. Perinatal death is reminiscent of the Sedaghatian spondylometaphyseal dysplasia disorder in humans, which is caused by pathogenic variants in the gene encoding the selenoprotein and key ferroptosis regulator *glutathione peroxidase 4* (*GPX4*). Protein expression levels of distinct selenoproteins in *Sepsecs*$^{Y334C/Y334C}$ mice were found to be generally reduced in brain and isolated cortical neurons, while transcriptomics analysis uncovered an upregulation of NRF2-regulated genes. Crossbreeding of *Sepsecs*$^{Y334C/Y334C}$ mice with mice harboring a targeted mutation of the catalytically active Sec to Cys in GPX4 rescued perinatal death of *Sepsecs*$^{Y334C/Y334C}$ mice, showing that the cardio-respiratory defects of *Sepsecs*$^{Y334C/Y334C}$ mice were caused by the lack of GPX4. Like in *Sepsecs*$^{Y334C/Y334C}$ mice, selenoprotein expression levels remained low and NRF2-regulated genes remained highly expressed in these compound mutant mice, indicating that selenium-independent GPX4, along with a sustained antioxidant response are sufficient to compensate for dysfunctional Sec-tRNA$^{[Ser]Sec}$ biosynthesis. Our findings imply that children with pathogenic variants in *SEPSECS* or *GPX4* may even benefit from treatments that incompletely compensate for impaired GPX4 activity.

1. Introduction

Selenoproteins are characterized as proteins containing the rare proteinogenic amino acid selenocysteine (Sec), which differs from cysteine in just one atom, selenium (Se) replacing sulfur. Yet, both the biosynthesis of the Sec-loaded tRNA$^{[Ser]Sec}$ and the co-translational incorporation of Sec into the nascent polypeptide chain are highly complex processes. Sec is co-translationally incorporated in response to a UGA/Sec codon in their mRNA [1]. In eukaryotes, a stem loop-like secondary structure in the 3' untranslated region of the mRNA, known as selenocysteine incorporation sequence (SECIS) element, facilitates binding of SECIS-binding protein 2 (SECISBP2) to suppress translation termination and to afford Sec-incorporation at the UGA codon [2].

The essentiality of the trace element Se was first reported in vitamin

* Corresponding author. Institut für Biochemie und Molekularbiologie, Universitätsklinikum Bonn, Nussallee 11, 53115, Bonn, Germany.
E-mail address: uschweiz@uni-bonn.de (U. Schweizer).
present addresses: Dept. Medical Biochemistry and Biophysics, Karolinska Institutet, Stockholm, SE-17177, Sweden.
1 present addresses: 3. Medical Clinic, Klinikum rechts der Isar, Technische Universität München, Munich; Germany.

https://doi.org/10.1016/j.redox.2021.102188
Received 1 October 2021; Received in revised form 26 October 2021; Accepted 11 November 2021
Available online 12 November 2021

E− and Se-deficient rats and then uncovered to be a close functional cooperation between vitamin E and the selenoenzyme glutathione peroxidase 4 (GPX4) in reducing lipid peroxides in cellular membranes [3–5]. Se-deficiency has been associated with diseases in humans and livestock [6]. Organ systems that require adequate Se levels and expression of selenoproteins are the musculo-skeletal, nervous, hematopoietic, and endocrine systems [7–11]. Accordingly, the first Sec-containing enzymes discovered were glutathione peroxidase (GPX) s, iodothyronine deiodinases (DIO), thioredoxin reductases (TXNRD), and methionine sulfoxide reductase B1, all carrying Sec in their catalytic centers. Genomic analyses showed that the human and mouse genomes contain 25 and 24 genes encoding selenoproteins, respectively [12]. Through systematically targeting selenoproteins in the mouse, the functions of individual selenoproteins were elucidated and several selenoproteins were found to be essential for mouse development. Initially, it was proposed that the roles of selenoenzymes were mainly concerned with the reduction of peroxides and other oxidized molecules, and in fact several selenoprotein-deficient mouse models showed an induction of nuclear factor erythroid 2–related factor 2 (NRF2)-regulated genes, including Se-independent peroxidases and glutathione-S-transferases [13–15]. The role of Sec in other selenoproteins, however, appears to be more diverse with Sec serving transport, structural or regulatory roles, although peroxidase functions on undefined substrates are still possible [7,16–18].

Through human genetics, an increasing number of individuals are being diagnosed with inborn errors of selenoprotein biosynthesis or with pathogenic variants in genes encoding selenoproteins [19], further highlighting the importance of selenoprotein function for human health. Pathogenic variants in the selenoprotein biosynthesis factor SECISBP2 cause endocrine, musculo-skeletal and immunological symptoms [20,21]. In contrast, pathogenic variants in selenocysteine synthase (SEPSECS), the enzyme catalyzing the last step in Sec-tRNA$^{[Ser]Sec}$ biosynthesis, mainly affect the nervous system and, depending on the variant, cause fatal neurodegeneration. For instance, the homozygous p.Y334C variant in *SEPSECS* causes progressive cerebello-cerebral atrophy in children, a neurodegenerative disorder now called pontocerebellar hypoplasia type 2D (PCH2D) [22,23]. SEPSECS is a vitamin B_6-dependent enzyme that binds phospho-seryl-tRNA$^{[Ser]Sec}$ and uses selenophosphate to convert it to Sec-tRNA$^{[Ser]Sec}$ [24,25]. Pathogenic variants in this enzyme thus generally limit the availability of Sec-tRNA$^{[Ser]Sec}$ for selenoprotein biosynthesis. It remains an open question why pathogenic variants in two genes in the same pathway cause two apparently different syndromes with either predominantly endocrine or neurological symptoms.

Results from gene targeting in mice and phenotypes of humans with pathogenic variants in respective genes are similar [9]. However, there are also notable differences: inactivation of the *Gpx4*, *Txnrd1*, *Txnrd2*, *Selenot*, and *Selenoi* genes in mice is early embryonic lethal [26–33]. Patients carrying homozygous pathogenic variants causing premature termination in *GPX4* are born, but are diagnosed with Sedaghatian spondylometaphyseal dysplasia and die of cardio-respiratory failure [34]. Patients carrying pathogenic variants in *TXNRD2* show isolated congenital glucocorticoid deficiency [35], and patients with pathogenic variants that reduce the activity of TXNRD1 show generalized seizures [36]. Likewise, inactivation of *Secisbp2* in mice is embryonic lethal, while neuron-specific inactivation of *Secisbp2* leads to neurological deficits [15,37]. However, neurological phenotypes are not a general finding in patients carrying pathogenic variants in *SECISBP2* [38].

In order to better understand the consequences of *SEPSECS*-deficiency, we have generated a *Sepsecs*$^{Y334C/Y334C}$ mouse model. These mice are born at the expected Mendelian frequency, but exhibit cardio-respiratory failure and die during the first day of life. This observation resembles patients with Sedaghatian disease caused by lack of GPX4 activity. We rescued *Sepsecs*$^{Y334C/Y334C}$ mice with transgenic expression of *Gpx4*^{Cys}, in which the Sec codon is replaced by a SEPSECS-independent Cys codon [39]. Such mice still show impaired selenoprotein expression and induction of NRF2-target genes in the heart and in the brain, but demonstrate that the selenoprotein most acutely needed after birth is GPX4. These findings may have consequences for attempts to treat inborn disorders of selenoprotein expression.

2. Material and methods

Nomenclature of selenoproteins follows the conventions as described in Gladyshev et al. [40].

2.1. Construction of targeting vectors by recombineering in bacteria

The methodology used was recently described [41]. Briefly, homologous arms (5' (exon 5) and 3' (exon 10)) were amplified by PCR using a BAC vector containing the *Sepsecs* gene (Source Bioscience) as a template. Primers used for PCR (see Table S1) contained the following restriction sites (*Xho*I and *Cla*I for exon 5 and *Cla*I and *Xma*I for exon 10) to facilitate subcloning into pGEMT-Easy vector (Promega). Both homologous arms were subsequently cloned stepwise into pDTA vector as detailed in Fig. S1. The mutation p.Y334C in exon 8 was introduced by site-direct mutagenesis following the manufacturer's instructions (QuikChange II Site-Directed Mutagenesis Kit, Agilent Technologies). Two silent mutations (p.I324 and p.T325) were also introduced upstream of the p.Y334C mutation in order to create an *Acl*I restriction site, which facilitates subsequent genotyping. Finally, these arms were cloned stepwise into pFRT Dual Neo vector to create pFRT Dual Neo_*Sepsecs*_Y334C vector.

Recombineering in DH10B bacteria containing the BAC_*Sepsecs* vector, the mini λ Tet plasmid, and the pDTA vector introduced the *Sepsecs* sequence from exon 5 to exon 10 into the pDTA vector (pDTA_*Sepsecs*_e5-e10) (See Fig. S1). DH10B bacteria containing pDTA_*Sepsecs*_e5-e10 vector and the mini λ Tet plasmid were transformed with pFRT Dual Neo_*Sepsecs*_Y334C. Another recombination step introduced the Y334C point mutation and the neo-cassette into pDTA_*Sepsecs*_e5-e10 vector to finally create the construct named pDTA_*Sepsecs*_e5-e10_FRT Dual Neo_*Sepsecs* _Y334C (Fig. S1). This construct was linearized with *Pac*I and electroporated into ES cells to create our mouse model.

2.2. Generation of the mouse models

Generation, breeding, and analyses were done under permits by state authorities G0176/07 (LAGESO Berlin), AZ 02.04.2014.A436, and 81–02.04.2019.A447 (LANUV Recklinghausen) according to EU Directive 2010/63/EU for animal experiments.

IDG 3.2 murine hybrid ES cells (129S6/SvEv/Tac x C57Bl/6J) were electroporated with 30 μg of linearized targeting vector, pDTA_*Sepsecs*_e5-e10_FRT Dual Neo_*Sepsecs* _Y334C. Fifty neomycin-resistant ES cell clones were analyzed by Southern-blotting. Based on the karyotype, one ES clone was microinjected into *C57*BL/*6* blastocysts. Genotyping of offspring from male chimeras and *C57*BL/*6* females confirmed germline transmission. The selection cassette was removed by breeding heterozygous mice with a FLP-deleter mouse. *Gpx4*$^{+/Cys}$ mice have been described previously [39] and were crossed with *Sepsecs*$^{+/Y334C}$. The *Sepsecs*^{Y334C} allele was also backcrossed for 5 generations on a 129Sv background. All *Sepsecs*$^{Y334C/Y334C}$ pups had the same phenotype as on the *C57*BL/*6* genetic background, and all subsequent analyses were performed with mice from the *C57*BL/*6* line.

2.3. Southern-blot

The procedure was carried out similarly as described in Ref. [41]. Briefly, 10 μg of genomic DNA from ES cell clones were digested with *Swa*I and *Eco*RV. After electrophoresis, DNA was depurinated and transferred to a nylon membrane (Hybond-N+, GE Healthcare)

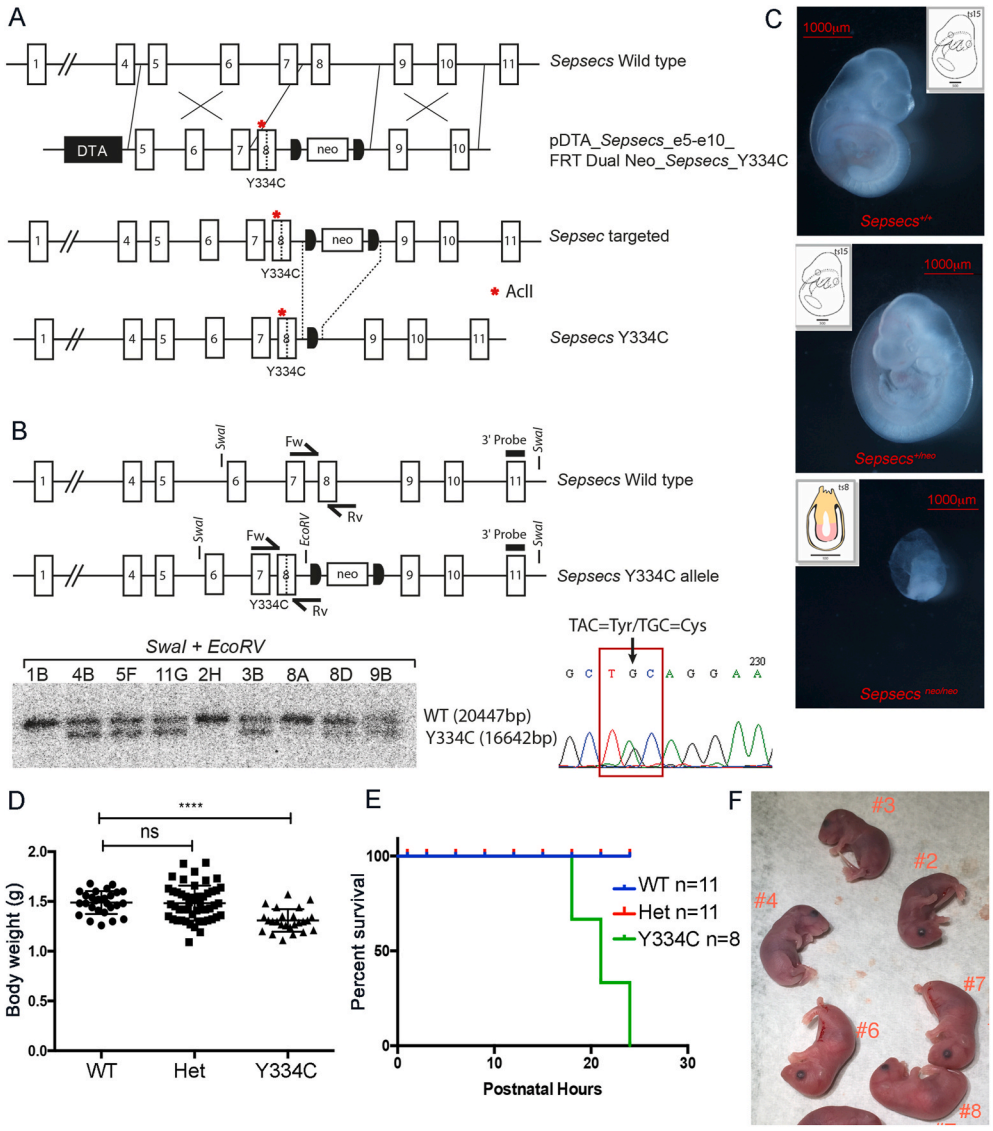

Fig. 1. Generation and phenotype of the *Sepsecs*^{Y334C} mice. A) Schematic of homologous recombination between the *Sepsecs* wild type allele and the targeting construct containing the p.Y334C mutation in exon 8 with a nearby *neo*-cassette flanked by two FRT sites in ES cells. A diagnostic *AclI* restriction site is represented by a red asterisk. The *neo* transgene was removed *in vivo* by mating with a *FLPe*-transgenic mouse creating the *Sepsecs* p.Y334C allele. B) Characterization of correct gene targeting by Southern-blot and Sanger sequencing. *SwaI* and *Eco*RV used for digestion of genomic DNA are displayed as well as the external probe (exon 11) and the primers used for DNA sequencing. Southern blot picture of several ES clones. The upper band corresponds to the wild type allele (20447bp) and the lower band (16642bp) to the targeted allele (*Sepsecs*^{neo}), respectively. Sanger chromatogram showing the heterozygous point mutation c.1001A > G resulting in the p.Y334C replacement. C) Pictures of embryos born from heterozygous mating between *Sepsecs*$^{+/neo}$ mice. *Sepsecs*$^{neo/neo}$ embryos showed developmental arrest in Theiler stage (TS) 8 compared with wild-type and heterozygous embryos that progressed to TS15. D) Body weights of newborn pups. Two-tailed *t*-test showed significant difference (p-value < 0,0001) between wild-type (WT) and *Sepsecs*$^{Y334C/Y334C}$ (Y334C) mice. *Sepsecs*$^{+/Y334C}$ are labelled as Het. E) *Sepsecs*$^{Y334C/Y334C}$ pups failed to survive beyond 24 h. F) Picture of cyanotic *Sepsecs*$^{Y334C/Y334C}$ mice (numbers = 2,3,4) compared to wild-type littermates (numbers = 6,7,8). (For interpretation of the references to color in this figure legend, the reader is referred to the Web version of this article.)

overnight. After cross-linking, the membrane was prehybridized with Church buffer for 1h at 65 °C. The 3′Probe was cloned from BAC_Sepsecs vector into pGEMT-Easy vector using the primers in Table S1. Fifty μCi of [α-^{32}P]dCTP (PerkinElmer) and Prime-It RmT random primer labeling kit (Agilent Technologies) were used to label the probe. Unincorporated labelled nucleotides were removed using Illustra microspin G-50 columns (Ge Healthcare). After hybridization overnight, the membrane was washed three times at 65 °C. Exposure for two days allowed visualization using a BAS 1800 II phosphoimager (Fujifilm).

2.4. Western-blot

50 μg of protein in RIPA buffer with protease and phosphatase inhibitors (Roche) were electrophoresed through a SDS-polyacrylamide gel and transferred onto a nitrocellulose membrane (GE Healthcare). Transfer was confirmed by Ponceau staining. Membrane blocking was performed following the recommendations of antibody suppliers. Antibodies and dilutions used for this study are listed in Table S2 (Supplemental material). Detection was performed by Fusion Solo imaging system (Vilber Lourmat Deutschland GmbH) using horseradish peroxidase (HRP) conjugated anti-rabbit or anti-mouse antibodies (Jackson Immunotech) and the enhanced HRP chemiluminescence substrate SuperSignal ™ West Dura (Thermo Fisher Scientific).

2.5. Alcian blue-Alizarin red staining

After removing the skin and organs, specimens were fixed in 95% ethanol for 4 days. Then they were stained with Alcian blue solution (0.03% Alcian blue; 80% ethanol; 20% acetic acid) for 3 days. After keeping the specimens for 8 h in 95% ethanol, they were rocked in a solution of 95% ethanol and 2% KOH for 16 h. This solution was replaced by Alizarin red solution (0.03% Alizarin red, 1% KOH) for 24 h. Skeletons were cleared in clearing solution (1% KOH; 20% glycerol) for 5 days. After that, the skeletons were transferred to a solution of 1:1 glycerol:95% ethanol for 1 day. Finally, the skeletons were preserved in 100% glycerol until pictures were taken and the lengths of bones were measured using NIS elements BR software (Nikon).

2.6. Hematoxylin and eosin staining

Hearts from pups were dissected and kept for 1 h in 4% PFA. Tissue was dehydrated and embedded in paraffin. Sections of 4 μm were cut with a microtome (Leica RM2555). After deparaffination, tissue was stained with hematoxylin and eosin. Pictures were taken and the wall thickness of the left ventricle was measured using NIS elements BR software (Nikon).

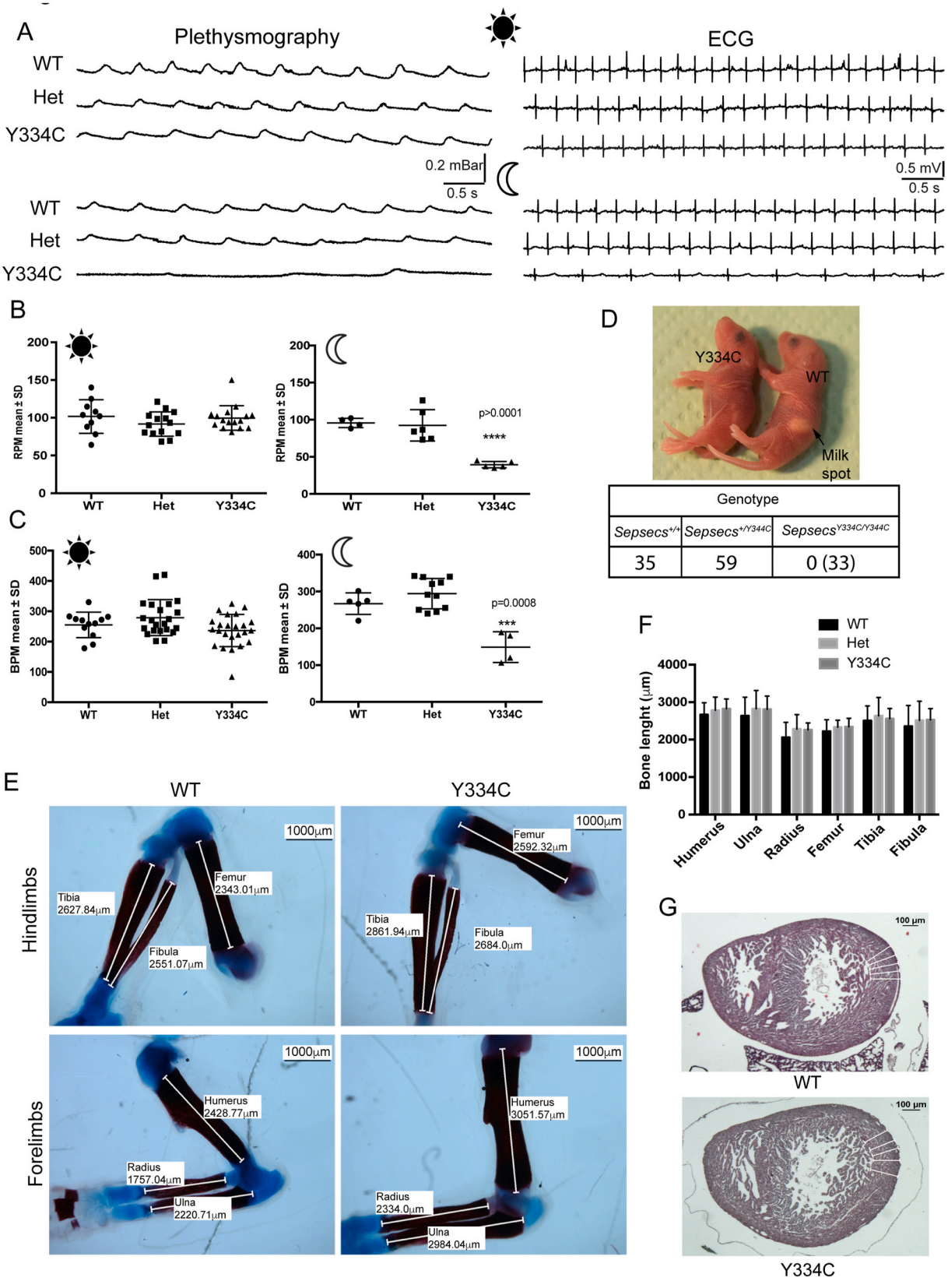

(caption on next page)

Fig. 2. Phenotypic features of *Sepsecs*$^{Y334C/Y334C}$ mice. A) Representative plethysmograms (left) and electrocardiograms (right) of wild-type (WT), *Sepsecs*$^{+/Y334C}$ (Het) and *Sepsecs*$^{Y334C/Y334C}$ (Y334C) newborn mice in the morning (sun symbol) and in the evening (moon symbol) of postnatal day 1. *Sepsecs*$^{Y334C/Y334C}$ pups showed no differences within the first hours after birth. However, differences of *Sepsecs*$^{Y334C/Y334C}$ pups are evident when they became cyanotic towards the end of their first day of life. Infrequent and shallow breathing as well as bradycardia and low QRS voltage in *Sepsecs*$^{Y334C/Y334C}$ mice compared to their litter-mates. B) Respiration rate was measured at midday (sun symbol) and in the evening (moon symbol) of postnatal day 1. RPM: respirations per minute. One-way ANOVA. SD: standard deviation. C) Heart rate was calculated at the same time points as in B. BPM: beats per minute. One-way ANOVA. D) Absence of milk spots in *Sepsecs*$^{Y334C/Y334C}$ pups (Y334C, arrow). E) Representative pictures of limbs from wild type (WT) and *Sepsecs*$^{Y334C/Y334C}$ (Y334C) pups stained with alcian blue and alizarin red. Alcian blue stains cartilage and alizarin red stains bone. Lengths of femur, tibia, and fibula and the lengths of humerus, radius and ulna, were determined. Scale is indicated in each picture as well as the length of each bone in micrometers. F) Bone lengths were not significantly different among genotypes. Means ± standard error of the mean. Numbers of animals are represented in the graph. G) Representative hematoxylin-eosin staining of cardiac ventricles from wild-type and *Sepsecs*$^{Y334C/Y334C}$ pups on P1. White bars represent measurements of the left ventricular wall thickness. No difference in left ventricular wall thickness was found between genotypes. (For interpretation of the references to color in this figure legend, the reader is referred to the Web version of this article.)

2.7. Cortical neuron culture

The procedure to prepare cortical neuron cultures from individual pup cortices was adopted from Beaudoin et al. [42].

2.8. Astrocyte culture

Astrocytes were cultured as described in Ref. [43]. Briefly, brains from newborn pups were dissected. Cortices were minced and mechanically disaggregated in DMEM-F12 supplemented with 10% FCS and 1% penicillin/streptomycin (Lonza). Cells were cultured in poly--L-Lysine coated flasks (TPP) for 15 days. Flasks were shaken overnight in order to detach microglial cells. Astrocytes were subcultured in 100 mm plates before they were treated with PLP and sodium selenite (Sigma).

2.9. ^{75}Se-labeling

The procedure was performed as described in Ref. [39]. Neuron cultures grown in 100 mm plates (TPP, Switzerland) were labelled with 10 μCi/plate of radioactive $Na_2[^{75}Se]O_3$ (Polatom) overnight. Cell lysates were collected with RIPA buffer. Electrophoresis in SDS-PAGE was performed with 50 μg of protein. To ascertain equal loading, the gel was stained with Coomassie brilliant blue. The gel was dried (gel dryer (Bio-Rad)) and exposed to a Phosphoimager screen. The autoradiography was developed by a BAS-1800 II Phosphoimager (Fujifilm).

2.10. Plethysmography and electrocardiogram

Plethysmography was performed by placing newborn pups into a 5 ml chamber (syringe) connected to a pressure sensor. Adult mice were weighed and anesthetized with ketamine-xylazine at 100 and 10 mg/kg, respectively before plethysmography in a 50 ml chamber. Transduced signals were amplified using a Dual Bio Amp amplifier (AD Instruments) and digitized using Power Lab 4/26 DAQ hardware and Lab Chart 8 software (AD Instruments). Pups were acclimatized to the testing environment, before measurements were recorded for 5 min. No acclimatization was necessary for adult mice. Since pups were unrestrained, pressure changes due to movements were noted and excluded from the

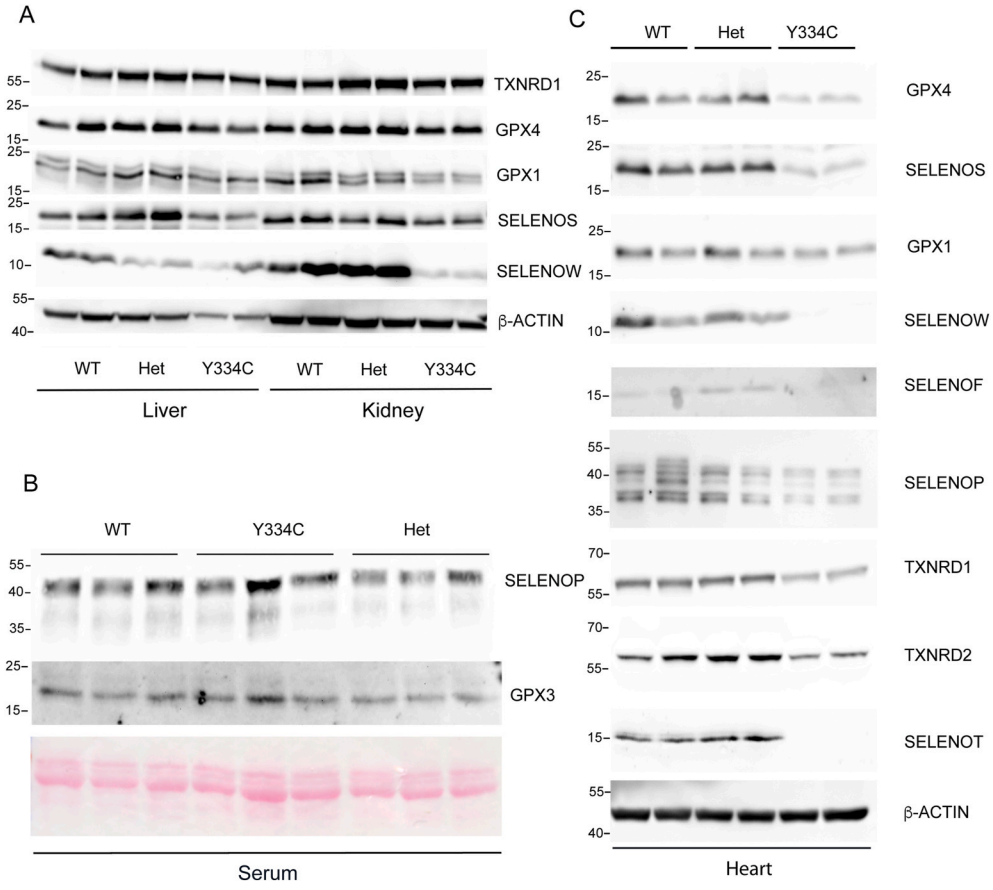

Fig. 3. Selenoprotein expression in *Sepsecs*$^{Y334C/Y334C}$ mice is tissue dependent. A) Liver and kidney lysates from wild-type (WT), heterozygous (Het) and homozygous (Y334C) newborn pups were assessed for the expression of several selenoproteins. Beta-actin was used as loading control. B) Analysis of serum selenoproteins (SELENOP and GPX3). Ponceau red was used as loading control. C) Expression of selenoproteins in hearts from newborn mice. Beta actin was used as loading control. (For interpretation of the references to color in this figure legend, the reader is referred to the Web version of this article.)

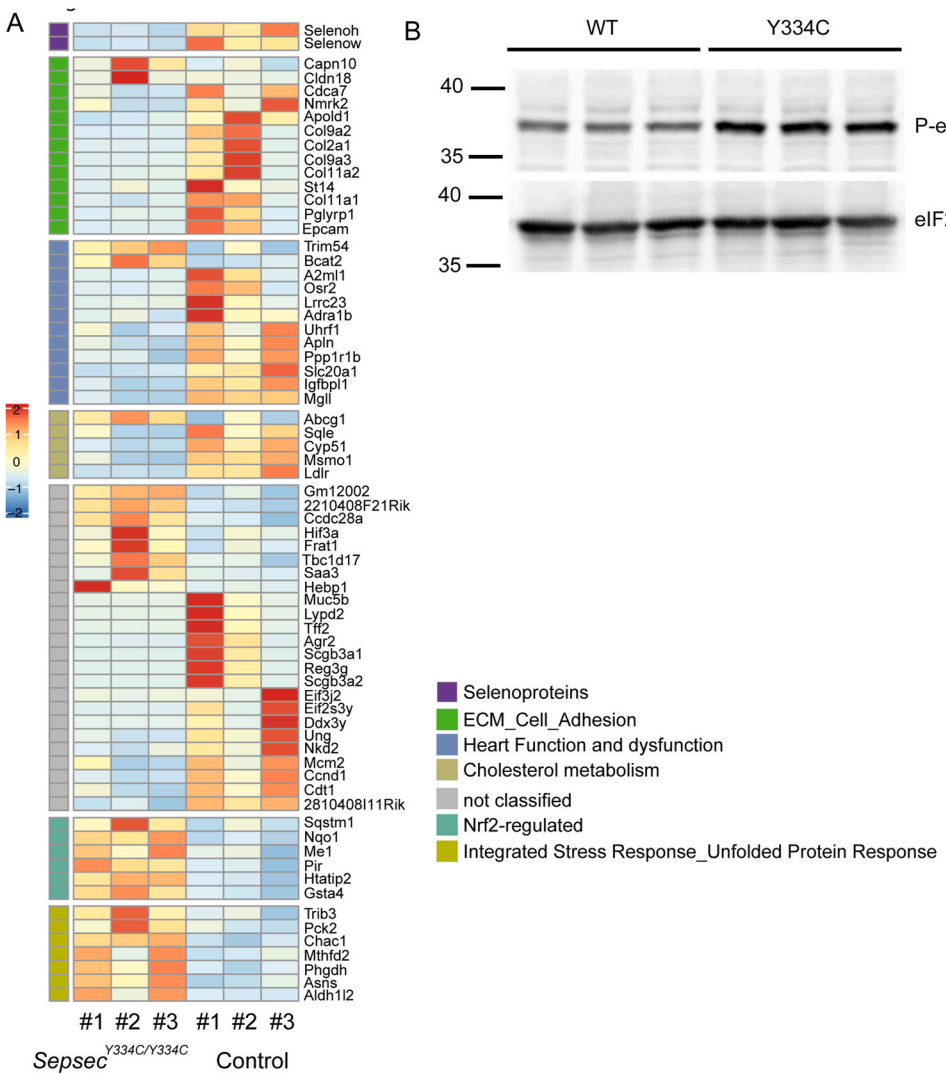

Fig. 4. Regulated pathways in *Sepsecs*$^{Y334C/Y334C}$ hearts determined by differentially expressed genes A) Heatmap of differentially expressed genes in heart of *Sepsecs*$^{Y334C/Y334C}$ mice compared with wild type. N = 3 per genotype. Up-regulated and down-regulated genes are indicated in red and blue, respectively. Regulated pathways are indicated by color code. B) Increased phosphorylation of eIF2α in hearts of *Sepsecs*$^{Y334C/Y334C}$ (Y334C) pups compared to wild-type (WT). Total eIF2α showed equal loading. . (For interpretation of the references to color in this figure legend, the reader is referred to the Web version of this article.)

respiration rate analysis. Pups that moved constantly were removed from the chamber and a second attempt was performed.

2.11. RNA extraction and sequencing

RNA from different mouse tissues was extracted using Trizol (Invitrogen) following the manufacturer's instructions.

3′-mRNA sequencing was performed by the Next Generation Sequencing (NGS) Core Facility of the Medical Faculty of the University of Bonn. Libraries were prepared using the QuantSeq 3′-mRNA-Seq Fw. Library Prep Kit (Lexogen, New Hampshire, United States) and the data was preprocessed using the options recommended by the manufacturer. Quality control was performed using fastqc v0.11.8. STAR aligner 2.6.0a (using the options recommended by the manufacturer) was used for alignment against the GRCm38 mouse (Ensembl release 102) genome retrieved from Ensembl. Raw data and raw counts can be obtained from GEO (GSE181852). The R-package DESeq2 was used for statistical analysis, as recommended by the provider (normalization of raw counts, dispersion estimation and negative binomial Wald test with Benjamini-Hochberg multiple test correction). Adjusted p-values < 0.05 were defined as significant.

3. Results

3.1. The pathogenic variant p.Y334C in the murine Sepsecs gene causes perinatal lethality

To recapitulate the human pathogenic variant in the murine *Sepsecs* gene [22], we introduced the p.Y334C variant into exon 8 of the murine *Sepsecs* locus at a position that is conserved among mammals/vertebrates (Fig. 1A–B). For gene targeting, an *FRT*-flanked *neomycin-phosphotransferase II* (*neo*) gene was inserted into intron 8, along with its own promoter and polyadenylation signal. Mice retaining the *neo* gene are designated *Sepsecs*^{neo}. Intercrosses of *Sepsecs*$^{+/neo}$ mice never yielded viable offspring with a *Sepsecs*$^{neo/neo}$ genotype (17 litters; 36 *Sepsecs*$^{+/+}$; 68 *Sepsecs*$^{+/neo}$; 0 *Sepsecs*$^{neo/neo}$, expected were 35). We therefore isolated embryos from these matings and found that *Sepsecs*$^{neo/neo}$ embryos remained arrested at Theiler stage (TS) 8 on embryonic day 8, while *Sepsecs*$^{+/neo}$ and wild-type littermates developed normally to reach TS15 on the same day (Fig. 1C). The early embryonic failure is reminiscent of mice carrying homozygous null mutations in *Secisbp2* [15], *Txnrd1* [29], *Txnrd2* [28], *Selenoi* [30], *Selenot* [33], and *Gpx4* [26,27,31,44] suggesting that the *neo* gene in intron 8 disrupts the function of the *Sepsecs* gene. Upon FLPe-mediated removal of the *neo* gene and associated sequences (Fig. 1A), *Sepsecs*$^{+/Y334C}$ mice were intercrossed, and these matings yielded life born *Sepsecs*$^{Y334C/Y334C}$ mice close to the expected Mendelian ratio (33 *Sepsecs*$^{Y334C/Y334C}$ mice out of

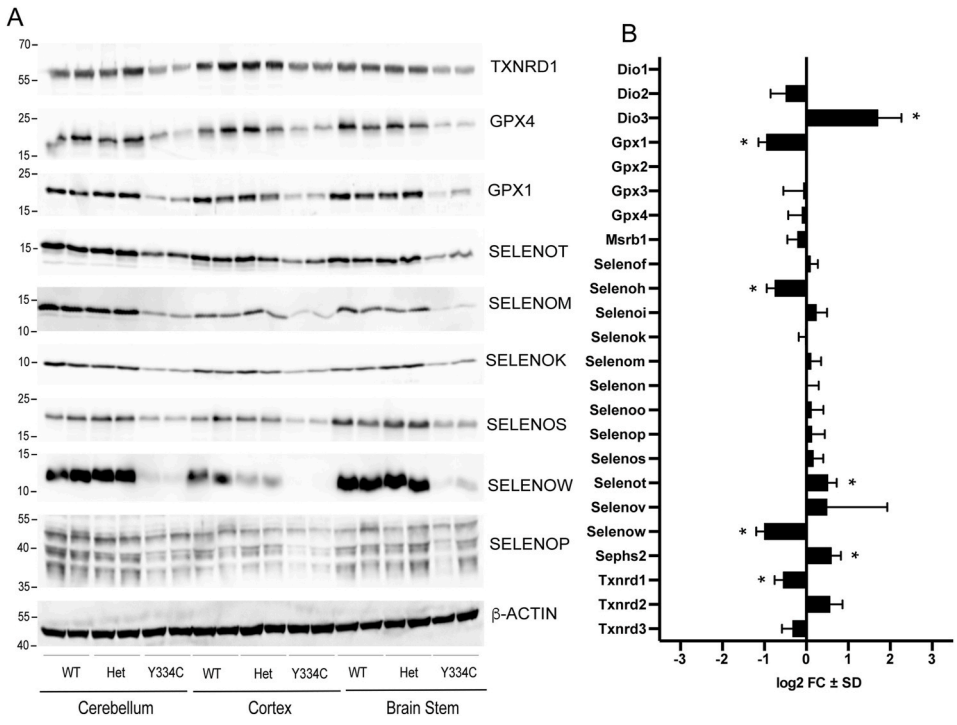

Fig. 5. Brain selenoprotein expression is severely affected in *Sepsecs*$^{Y334C/Y334C}$ mice. A) Analysis of selenoprotein expression in different brain regions (cortex, cerebellum and brain stem) from newborn mice. Beta-actin shows equal loading. B) Relative abundance of selenoprotein-related reads from cortex of *Sepsecs*$^{Y334C/Y334C}$ newborns compared to controls. N = 3 per genotype. *q < 0.05, BH Correction. Means ± standard deviation.

127 life-born pups). *Sepsecs*$^{Y334C/Y334C}$ pups had a 12 ± 8.8% decreased body weight at birth (Fig. 1D) and all p.Y334C homozygous pups invariably died during their first day of life, after becoming cyanotic (Fig. 1E and F).

This phenotype is reminiscent of the cardio-respiratory failure of children with a homozygous pathogenic variant leading to premature termination in the gene encoding the selenoprotein glutathione peroxidase 4 (*GPX4*) [34]. We therefore assessed the breathing pattern of newborn mice by plethysmography at noon of the day of birth and in the late evening of the same day (Fig. 2A left panel and 2B). We found that *Sepsecs*$^{Y334C/Y334C}$ mice initially had normal breathing frequency at noon, but displayed shallow and irregular breathing at less than half of the frequency of wild-type and heterozygous litter mates at the end of the day (Fig. 2A and B). Electrocardiography showed that the heart rate of the homozygous mutant pups was not different from controls when measured several hours after birth, but decreased later on the same day when cyanosis occurred (Fig. 2A right panel and 2C). This observation is compatible with an atrio-ventricular block caused by hypoxia, although we did not attempt to further investigate the exact pathomechanism of bradycardia. Another observation was the absence of "milk spots" in *Sepsecs*$^{Y334Y/Y334C}$ mice (Fig. 2D). Milk spots are the visible filling of the stomach with milk in postnatal pups. While all litter-mates showed the milk spot, none of the 33 *Sepsecs*$^{Y334C/Y334C}$ mice did. Absence of a milk spot might indicate an inability to suckle, i.e. a dysfunction of motoneurons or muscular weakness. We ruled out the alternative explanation that mothers abandoned their homozygous pups after birth. The absence of suckling may explain some of the body weight difference (Fig. 1D). An obvious phenotype in children born with Sedaghatian disease is the stunted growth of long bones [34,45]. We therefore stained the skeleton of newborn *Sepsecs*$^{Y334C/Y334C}$ mice with alizarin red and alcian blue and measured the lengths of the long bones of the limbs (Fig. 2E). In comparison to wild-type and heterozygous *Sepsecs*$^{+/Y334C}$ mice, homozygous *Sepsecs*$^{Y334C/Y334C}$ mice did not show any differences in bone length (Fig. 2F). Thus, we did not further investigate a potential phenotype in the cartilage. Previously we described perinatal death with failure to suckle of mice with a heart-specific inactivation of *Txnrd2* [28]. Histological analysis of hearts from *Sepsecs*$^{Y334C/Y334C}$ mice did not support the notion that reduced TXNRD2 activity leads to cardiac hyperthrophy, since left ventricular wall thickness remained unaltered in the mutant pups (Fig. 2G).

3.2. Organ-specific impact of the p.Y334C mutation on selenoprotein expression

We next asked how the p.Y334C variant in the *Sepsecs* gene may impact on the expression of selenoproteins in *Sepsecs*$^{Y334C/Y334C}$ mice. Western blot analysis of a panel of selenoproteins at postnatal day 1 revealed surprisingly little effect of the mutation in liver. SELENOW showed the clearest reduction among the selenoproteins analyzed, although this effect was modest. In kidney the effect was clearer, although selenoproteins like GPX4 still only showed a moderate reduction (Fig. 3A). Liver and kidney secrete two plasma selenoproteins, SELENOP and GPX3, respectively, and expression of both was not reduced in the homozygous *Sepsecs*$^{Y334C/Y334C}$ mice according to immunoblot analysis (Fig. 3B). While seemingly surprising at first glance, these findings are in line with the clinical descriptions of patients with pathogenic variants in the *SEPSECS* gene, which are not reported to have hepatic or renal phenotypes. By stark contrast, in the heart the effect of the homozygous p.Y334C *Sepsecs* variant was much more prominent: not only was SELENOW almost undetectable, also SELENOF and SELENOT were strongly reduced (Fig. 3C). Moreover, even selenoproteins with the Sec in the penultimate position, like SELENOS, TXNRD1 and TXNRD2 were clearly reduced. GPX1 was again surprisingly little affected, while there was a clear reduction in GPX4, as expected.

To further investigate the effects of reduced selenoprotein expression in the heart, we performed 3'mRNA sequencing. Plotting all significantly regulated genes into a heatmap revealed several pathways regulated in *Sepsecs*$^{Y334C/Y334C}$ hearts on postnatal day 1 (Fig. 4A). As expected, a number of selenoprotein mRNAs were reduced (*Selenoh*,

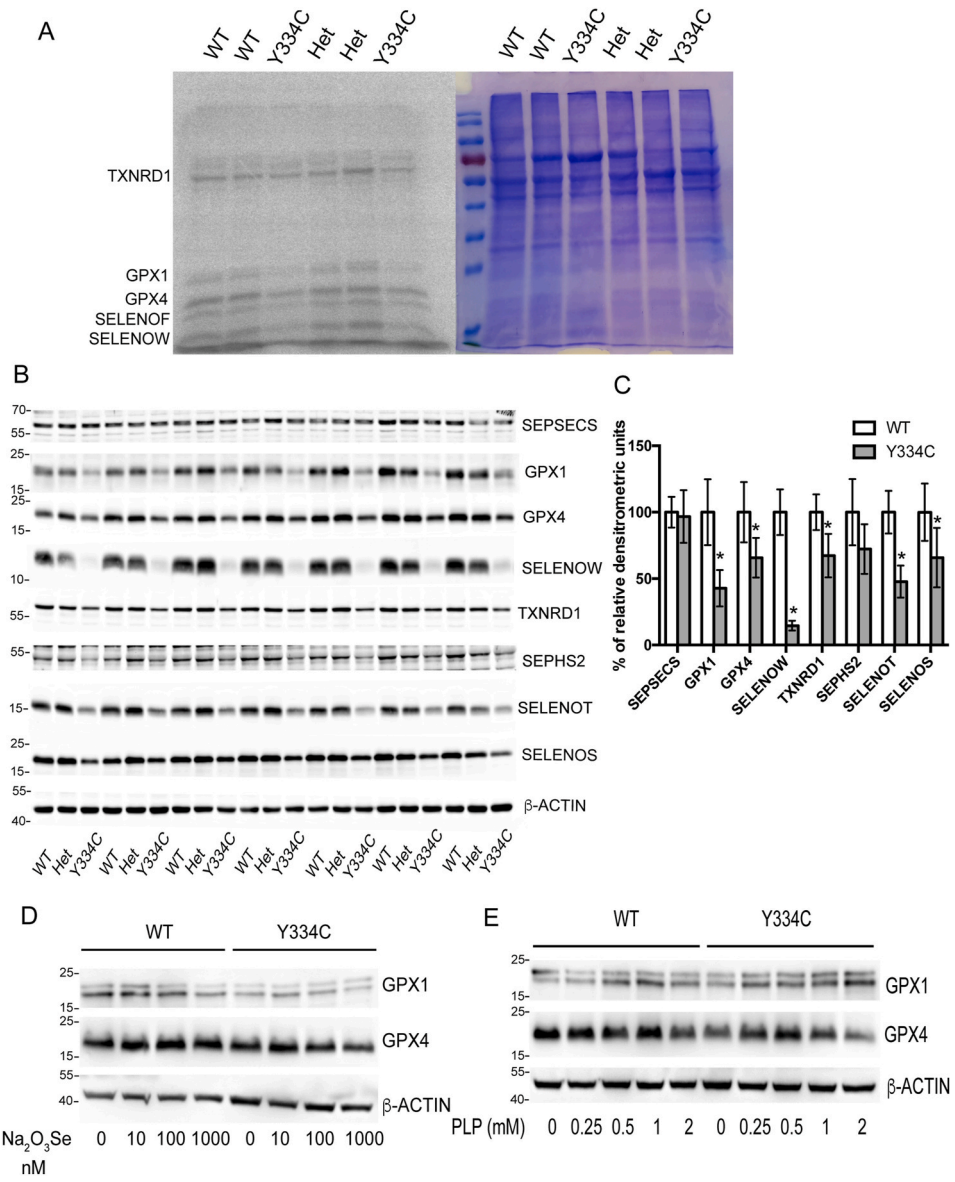

Fig. 6. Selenoprotein expression in neuron and astrocyte cultures. A) ^{75}Se metabolic labeling of wild-type (WT), heterozygous (Het) and homozygous mutant (Y334C) cortical neuron cultures. Coomassie blue staining shows equal loading. B) Selenoprotein expression of neuron cultures. Beta-actin shows equal loading. SEPSECS protein is detectable in homozygous *Sepsecs*$^{Y334/Y334C}$ mutant. C) Western blot quantification of neuronal selenoprotein expression. Student's *t*-test. Means ± standard deviation. $p_{(SELENOW)} = 2.3 \times 10^{-8}$, $p_{(SELENOT)} = 1.6 \times 10^{-5}$ $p_{(GPX1)} = 0.0001$, $p_{(TXNRD1)} = 0.001$, $p_{(GPX4)} = 0.005$, $p_{(SELENOS)} = 0.013$ D) and E) Representative selenoprotein expression of cultured astrocytes treated with Na_2SeO_3 (D) or PLP (E). Concentrations are indicated in the figure. Beta-actin was used as loading control. (For interpretation of the references to color in this figure legend, the reader is referred to the Web version of this article.)

Selenow). In agreement with the general impairment of selenoprotein translation, several NRF2-target genes, which are known to be induced under oxidative stress conditions, like *Nqo1* and *Gsta4*, were significantly induced. Additional NRF2-targets, such as the autophagy regulator p62/sequestome1 (*Sqstm1*), malic enzyme (*Me1*), *Htatip2* and the NF-κB activator Pirin (*Pir*), were significantly elevated [46]. Surprisingly, we observed changes in gene expression that imply a surplus of cellular cholesterol. Cholesterol biosynthetic genes, squalene epoxidase (*Sqle*), lanosterol-14-demethylase (*Cyp51*), and 4-Methylsterol-Demethylase (*Msmo1*) were significantly decreased. Moreover, the LDL-receptor (*Ldlr*), which is involved in cellular uptake of cholesterol, was repressed, whereas *Abcg1,* a cellular cholesterol exporter, was induced. While still unexplained, the link between cholesterol metabolism and selenoproteins has been noted before [47,48].

An interesting finding was the induction in *Sepsecs*$^{Y334C/Y334C}$ mice of genes associated with the unfolded protein response (UPR) and integrated stress response (ISR) pathways: *Trib3*, *Asns*, *Phgdh*, *Mthdf2*, *Chac1*, and *Pck2*. In support of this pathway, *Aldh1l2*, a mitochondrial N^{10}-formyl-tetrahydrofolate dehydrogenase, was induced. Consistent with a transcriptomic response to protein folding stress, Western blot of neonatal hearts showed substantially increased phosphorylation of eIF2α in the *Sepsecs*$^{Y334C/Y334C}$ mice (Fig. 4B). Activation of the UPR points to the deficiency of selenoproteins that are involved in protein folding and maturation in the ER (SELENOF, SELENOM, SELENOS, and SELENOT) [1], while induction of the ISR is compatible with mitochondrial stress previously observed in heart-specific *Txnrd2* deficient mice [28].

3.3. Skewed expression of distinct selenoproteins in brain regions and cultured neurons in Sepsecs$^{Y334C/Y334C}$ mice

The leading phenotype of human SEPSECS-deficiency is neurodegeneration, and neurodegeneration is a hallmark of severe selenoprotein deficiency in the brain [23,27,49–53]. We thus investigated selenoprotein expression by Western blot in the brains (cerebral cortex, cerebellum, and diencephalon/brain stem) of newborn mice using an expanded panel of antibodies. Expression of all tested selenoproteins was reduced in all brain regions in *Sepsecs*$^{Y334C/Y334C}$ mice, while *Sepsecs*$^{+/Y334C}$ mice showed no differences compared to wild-type (Fig. 5A). Consistent with a severe phenotype the essential selenoprotein GPX4 was profoundly reduced in all brain regions in the homozygous *Sepsecs* mutants (Fig. 5A). 3'mRNA sequencing of cerebral cortex corroborated

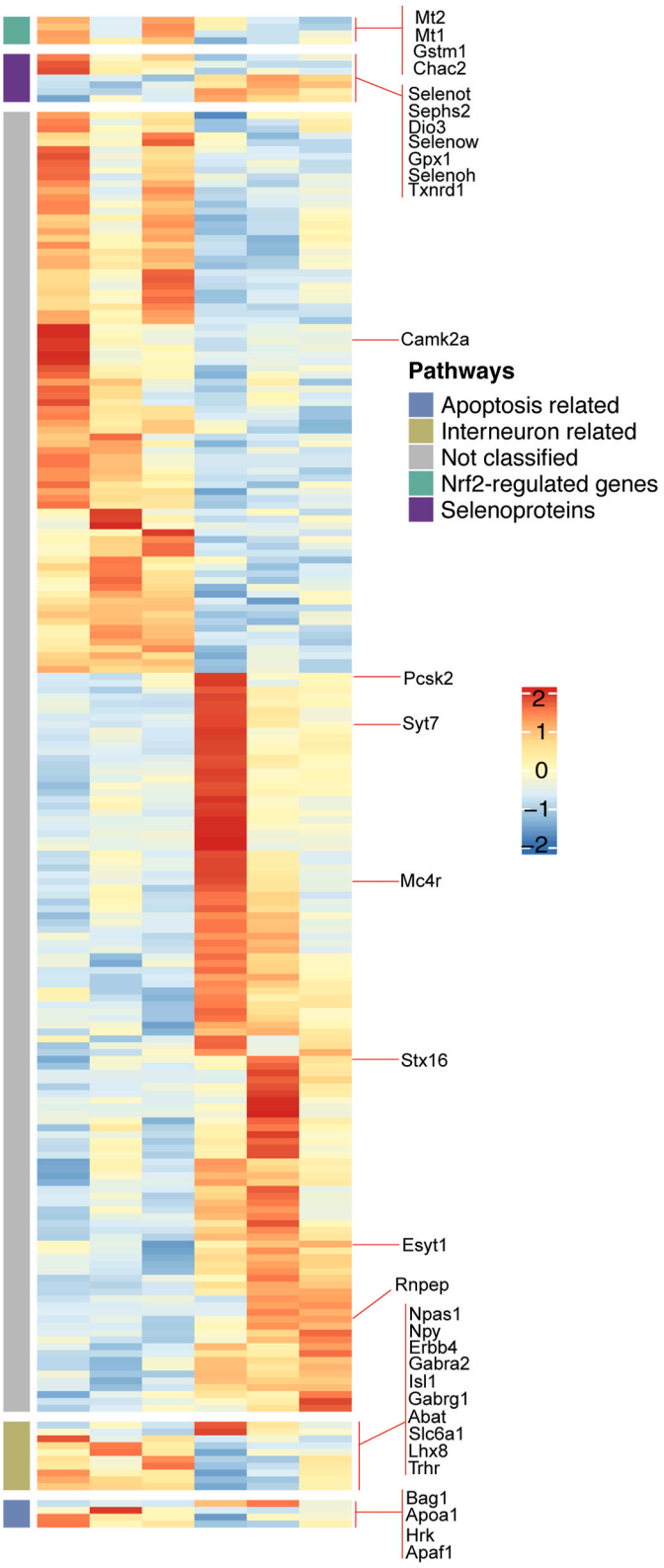

Fig. 7. Differentially expressed genes in cortex from *Sepsecs*$^{Y334C/Y334C}$ newborns. Heatmap showing the differentially expressed genes in cortex of Y334C homozygous mutants compared with wild-types. N = 3 per genotype. Up-regulated and down-regulated genes are indicated in red and blue, respectively. Associated pathways related to selenoproteins, (GABAergic) interneurons, NRF2-regulated genes, and apoptosis are indicated. (For interpretation of the references to color in this figure legend, the reader is referred to the Web version of this article.)

reduced levels of selenoprotein mRNAs (*Gpx1, Selenoh, Txnrd1* and *Selenow,* Figs. 5B and 7). Interestingly, several selenoprotein mRNAs including *Sephs2, Dio3,* and *Selenot* mRNAs were induced in the cortex of *Sepsecs*$^{Y334C/Y334C}$ mice, suggesting compensatory up-regulation (Figs. 5B and 7).

In order to substantiate the findings that cortical neurons are specifically affected in their selenoprotein biosynthesis in *Sepsecs*$^{Y334C/Y334C}$ mice, we metabolically labelled cultured cortical neurons with ^{75}Se-selenite (Fig. 6A). ^{75}Se-labelled bands were generally weaker in *Sepsecs*$^{Y334C/Y334C}$ neurons, with GPX4 being the least affected selenoprotein in line with its essentiality in neurons and with its well-established top position in the hierarchy among selenoproteins [54]. Immunoblot analysis in neurons supported these findings and showed that GPX1, SELENOT and SELENOW were significantly reduced. SEPHS2 was reduced, but missed significance (Fig. 6B and C). Next, we established primary astrocytes *in vitro* and supplemented the culture medium with 10–1000 nM sodium selenite in an attempt to rescue GPX1 expression. However, no such effect of selenite was observed (Fig. 6D). Since the position of the mutated Tyr334 in the protein structure is close to the binding site of PLP [55], we then asked whether the mutant protein might be impaired in PLP binding. To this end, we supplemented the astrocyte medium with up to 2 mM PLP and tested whether selenoprotein expression could be rescued; however, PLP supplementation failed to improve expression of GPX1 in *Sepsecs*$^{Y334C/Y334C}$ astrocytes (Fig. 6E).

3'mRNA sequencing of cerebral cortex prepared from newborn mice revealed a higher number of significantly regulated genes than in heart: As frequently observed in selenoprotein-deficient models, NRF2-dependent genes were induced, like *Gstm1, Mt1, Mt2,* and *Chac2* (Fig. 7). Consistent with earlier findings that the numbers of GABAergic neurons were affected in *Trsp*- and *Gpx4*-knockout mice [27,49], several genes associated with GABAergic signaling were differentially expressed. GABA-A receptor subunits were increased (*Gabra2*, *Gabrb2, and Gabrg1*) as were the GABA-degrading enzyme *Abat* and the vesicular GABA transporter *Slc6a1*, suggesting together an increase in GABAergic signaling. In addition, *Erbb4*, a marker of a subset of GABAergic interneurons was induced. Conversely, *Npas1*, a redox-sensitive transcription factor expressed specifically in GABAergic neurons, was reduced in the mutants. Other peptide co-transmitters, biosynthetic enzymes, and receptors were down-regulated, e.g. *Npy*, *Grp, Pcsk2, Rnpep and Mc4r*. Synaptic proteins synaptotagmin VII (*Syt7*), extended synaptotagmin 1 (*Esyt1*), and syntaxin 16 (*Stxn16*) were likewise reduced. Among the top genes found to be upregulated were *CamK2a*, *Trhr*, and the transcription factors *Isl1* and *Lhx8,* which are known to interact in the specification of cholinergic interneurons [56,57]. Induction of genes associated with apoptosis like harakiri (*Hrk*) and apoptosis inducing factor 1 (*Apaf1*) is consistent with a stress response. In this line, the anti-apoptotic gene *Bag1* was down-regulated. Many genes associated with cytoskeleton, extracellular matrix and neuronal pathfinding were affected, which is not surprising given the early developmental stage of the mice (Fig. 7). A transcriptional response to protein folding stress like in the heart was, however, not observed in the brain.

3.4. Perinatal lethality of homozygous *Sepsecs*$^{Y334C/Y334C}$ mice is rescued by transgenic expression of Se-independent GPX4^{Cys}

The strikingly similar clinical presentation of cardio-respiratory failure of *Sepsecs*$^{Y334C/Y334C}$ mice and patients with Sedaghatian disease, that carry pathogenic variants in the *GPX4* gene, suggested that isolated GPX4 deficiency could be the reason for the perinatal death of *Sepsecs*$^{Y334C/Y334C}$ mice. In order to directly address this question, we took advantage of a mouse strain harboring a site-directed replacement of the catalytically important Sec to Cys in the *Gpx4* allele (p.U46C; in the following referred to as *Gpx4*^{Cys}) [39]. *Gpx4*$^{+/Cys}$ mice are phenotypically normal [39]. We thus combined the *Gpx4*^{Cys} allele with the *Sepsecs*^{Y334C} line in order to create a mouse model in which the GPX4

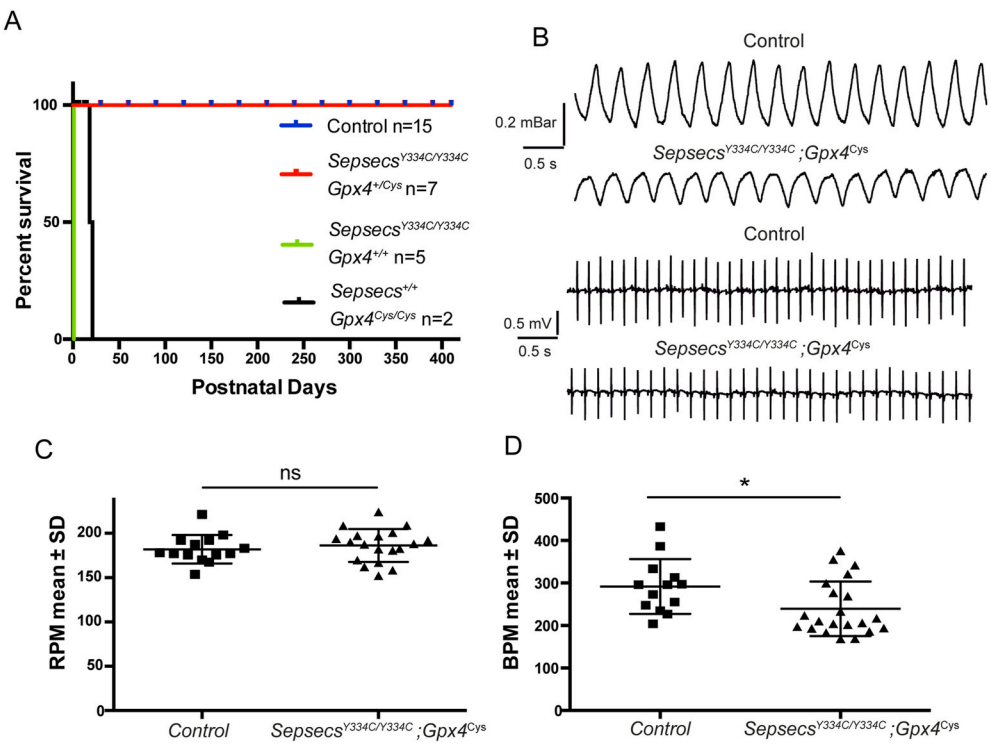

Fig. 8. Non-selenocysteine *Gpx4*^{Cys} expression fully rescues *Sepsecs*$^{Y334C/Y334C}$ mice from perinatal death. A) *Sepsecs*$^{Y334C/Y334C}$; *Gpx4*$^{+/Cys}$ mice (red line) survived at least one year, while *Sepsecs*$^{Y334C/Y334C}$; *Gpx4*$^{+/+}$ mice die prematurely (black line). *Sepsecs*$^{+/+}$; *Gpx4*$^{Cys/Cys}$ mice die around weaning as previously described [39]. *Sepsecs*$^{Y334C/Y334C}$; *Gpx4*$^{Cys/-Cys}$ mice were not born. B) Representative plethysmographs (upper panel) from *Sepsecs*$^{Y334C/Y334C}$; *Gpx4*$^{+/Cys}$ and *Sepsecs*$^{+/+}$; *Gpx4*$^{+/Cys}$ (control) mice shows similar respiration rate, but different tidal volume that may be associated with their 30% reduced body weight. Representative electrocardiograms (lower panel) from the same mice as in the upper panel. Scale is indicated. C) Respiration rate (RPM = respiration per minute) represented as mean ± standard deviation (SD) of *Sepsecs*$^{Y334C/Y334C}$; *Gpx4*$^{+/Cys}$ and control littermates. *Sepsecs*$^{+/+}$; *Gpx4*$^{+/Cys}$ were preferred as controls. However, any littermate non-homozygous for *Sepsecs* gene was used as control when the preferred ones were not available. D) Heart rate (BPM = beats per minute) of *Sepsecs*$^{Y334C/Y334C}$; *Gpx4*$^{+/Cys}$ and control littermates represented as Mean ± SD. Student's *t*-test p = 0.028. (For interpretation of the references to color in this figure legend, the reader is referred to the Web version of this article.)

activity would not be entirely dependent on Sec incorporation.

Remarkably, *Sepsecs*$^{Y334C/Y334C}$; *Gpx4*$^{Cys/+}$ mice were fully rescued from perinatal death, and seven mice already reached more than one year of age (Fig. 8A). Similar studies with identical results were performed with mice bred on the 129Sv genetic background (not shown). The only difference was that on the 129Sv genetic background *Gpx4*$^{Cys/Cys}$ mice were born, which are embryonic lethal on a C57Bl/6 background. Plethysmography showed normal breathing frequency of *Sepsecs*$^{Y334C/Y334C}$; *Gpx4*$^{Cys/+}$ mice (Fig. 8B and C), although the heart rate was slightly decreased (Fig. 8B, D). Therefore, we conclude that heart failure of *Sepsecs*$^{Y334C/Y334C}$ mice at postnatal day 1 is not caused by the lack of TXRND2 or any other selenoprotein, but is a result of the respiratory failure caused by GPX4 deficiency.

Given the profound stress response observed in neonatal *Sepsecs*$^{Y334C/Y334C}$ hearts (see Fig. 4), we wondered how gene expression might be changed in the hearts of adult *Sepsecs*$^{Y334C/Y334C}$ mice that have been rescued by a GPX4^{Cys} allele. To this end, we performed 3'mRNA sequencing analysis of hearts from mice at an age of 75 days. Overexpression of a large set of NRF2-responsive genes was evident in *Sepsecs*$^{Y334C/Y334C}$; *Gpx4*$^{Cys/+}$ mice (Fig. 9A). Among the significantly regulated genes were genes known to be related to heart function and regeneration like apelin. *Selenoh* and *Selenow* mRNA were decreased, while, interestingly, *Txnrd1* mRNA was induced. Western blot analysis confirmed impaired selenoprotein expression in the homozygous *Sepsecs* mutants, while the signal of GPX4 was enhanced because of the improved translation of GPX4^{Cys} over the Sec-containing enzyme (Fig. 9B). A persistent stress response was further demonstrated by an increased phosphorylation of eIF2α, although transcriptomic analysis did not demonstrate significant induction of UPR or ISR genes in this experiment as in the newborn hearts (Fig. 9C). In line with the stress response was the transcriptional induction of two genes associated with autophagy (*Sqstm1* and *Bnip3*). *Sqstm1* is also NRF2-regulated.

In the brain, selenoprotein expression followed the expected hierarchy, i.e. TXNRD1 and SELENOS were less affected by the *Sepsecs* mutation than GPX1, SELENOT, SELENOM, and SELENOW (Fig. 10A). Interestingly, *Selenop* was induced (Fig. 10B), possibly a response to reduced translation of selenoproteins [51]. As in the heart, transcriptomic analysis revealed an induction of NRF2-regulated genes (Fig. 10B). Genes involved in the UPR pathway or autophagy were not induced in the brain. In contrast, many genes associated with an immune response or inflammation were induced as previously seen in neuron-specific *Secisbp2*-mutant mice [41]: *C1q, C3, C4, Cxcl10, Ctss, Itgax, Cebpb*, but also *Gfap*, a marker of astrocytosis.

Among the downregulated genes were *Pde1b* and *Sipa1l1*, which are known to interact with CAMK2A (which is regulated on the mRNA level in newborn cortex, see Fig. 7) [58]. The same study reported an interaction of CAMK2A with GABAR1, which is regulated in newborn cortex as well.

Three genes including ethanolamine-phospho-lyase (*Etnppl*), sphingosine-1-phosphate-lyase (*Sgpl1*), and the lipid transfer protein *Stard10*, were transcriptionally regulated in *Sepsecs*$^{Y334C/Y334C}$; *Gpx4*^{Cys} cortex consistent with an adaption of phosphatidyl-ethanolamine metabolism to the lack of SELENOI, which is an ethanolamine phosphotransferase.

4. Discussion

We wanted to address the question why, in humans, pathogenic variants in *SEPSECS* lead to more severe disease than pathogenic variants in *SECISBP2*. To this end our laboratory created mouse models carrying pathogenic variants in both *Sepsecs* (this study) and *Secisbp2* [41]. Unfortunately, all these human pathogenic variants lead to more severe phenotypes in mice than in the respective human patients (see also [32]). We report here that the homozygous p.Y334C variant in *Sepsecs* leads to perinatal death in mice, while children with the same variant have reached several years of age [22]. The *Sepsecs* variant is clearly less functional *in vivo*, as mice show an overall reduction of selenoprotein expression in several organs, including heart and brain.

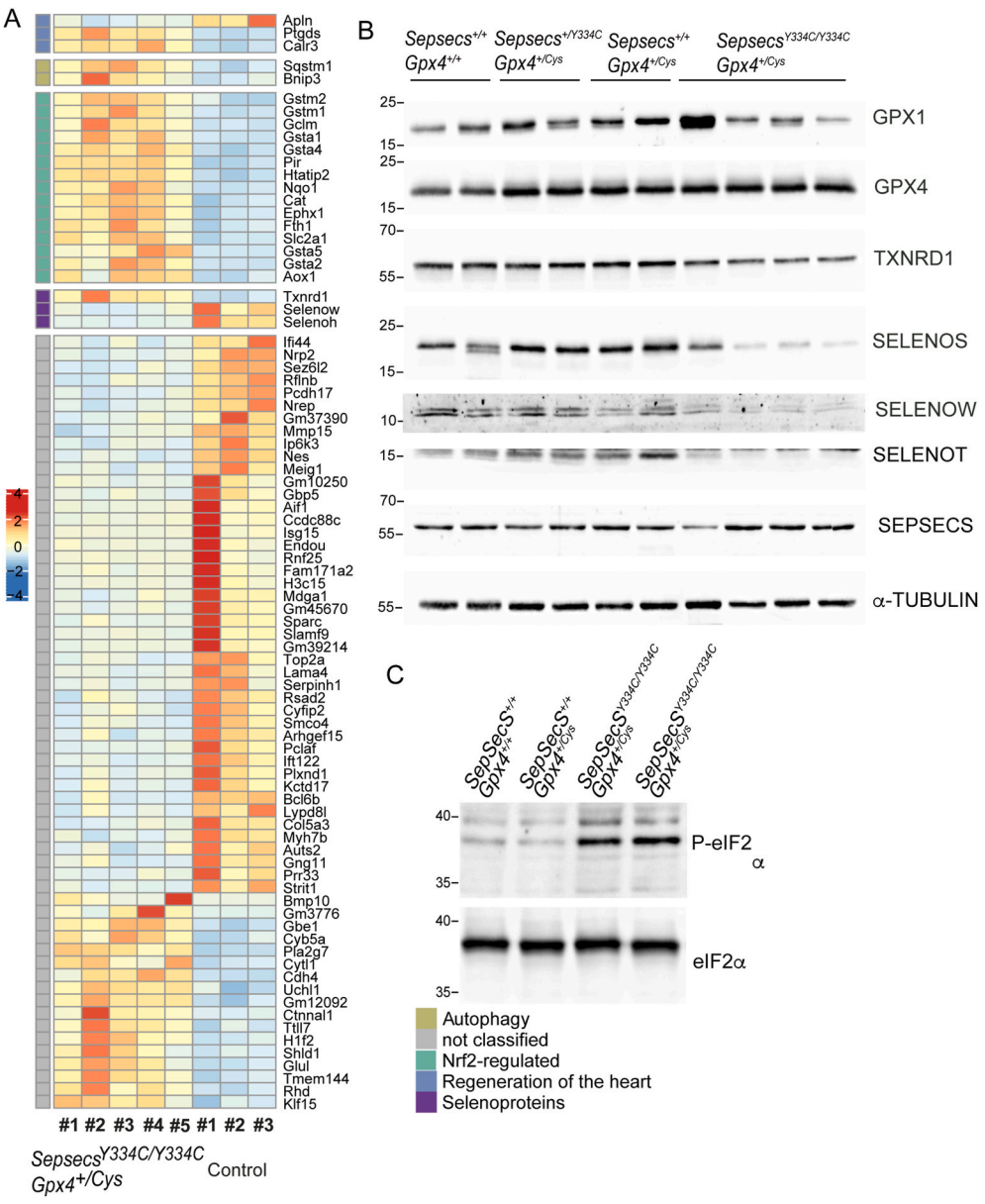

Fig. 9. Gene and protein expression of hearts from *Sepsecs*$^{Y334C/Y334C}$; *Gpx4*$^{+/Cys}$ mice. A) Heatmap showing significantly regulated genes from hearts of Sepsecs$^{Y334C/Y334C}$; Gpx4$^{+/Cys}$ mice (N = 5) versus control (N = 3). Up-regulated and down-regulated genes are indicated in red and blue, respectively. Selenoproteins and pathways (activated or inhibited) based on the regulated genes are indicated. B) Selenoprotein expression of the heart is shown according to the genotype. All animals were male. Wild-type, double heterozygous and *Gpx4*$^{+/Cys}$ mice are controls. SEPSECS expression is not altered. Beta-actin shows equal loading. C) Phosphorylated eIF2α is induced in the hearts of male *Sepsecs*$^{Y334C/Y334C}$ mice rescued with *Gpx4*$^{+/Cys}$. Total eIF2α shows equal loading. (For interpretation of the references to color in this figure legend, the reader is referred to the Web version of this article.)

The mice initially show normal heartbeat frequency and breathing pattern, but do not feed and then develop an irregular and shallow breathing pattern ultimately leading to cyanosis and cardio-respiratory failure at the end of their first day after birth. Such a phenotype was also described for mice with a heart-specific inactivation of *Txnrd2* [28]. Heterozygous variants in *TXNRD2* are over-represented in patients with dilated cardiomyopathy [59], and mice with a constitutive inactivation of *Txnrd2* show an embryonic heart defect [28]. Histological analysis of left ventricular wall thickness did not indicate a loss-of-function of TXNRD2 in *Sepsecs*$^{Y334C/Y334C}$ newborn mice (Fig. 2F). We then speculated that GPX4 may be the critical selenoprotein in *Sepsecs*$^{Y334C/Y334C}$ mice and genetically complemented the mice with a Se-independent *Gpx4*^{Cys} transgene. *Gpx4*^{Cys}-transgenic *Sepsecs*$^{Y334C/Y334C}$ mice were apparently fully rescued from perinatal death and grew to adulthood with normal breathing frequency and a slightly reduced heart rate. The rescue of perinatal lethality of *Sepsecs*$^{Y334C/Y334C}$ mice with the *Gpx4*^{Cys} allele was possible on two different genetic backgrounds. These findings suggest that the only critical selenoprotein is GPX4. GPX4 is known to be essential in mice and it collaborates with vitamin E in limiting lipid peroxidation and ferroptosis [4,5,60,61]. Ferroptosis may contribute to motoneuron death and thus impair feeding and breathing in the perinatal *Sepsecs*$^{Y334C/Y334C}$ mice [62].

The fact that the *Sepsecs* mutation reduces GPX4 expression below the threshold needed to survive, while even *null* mutations (in the brain and liver) in *Secisbp2* allow survival [15,37], suggest that a limited availability of Sec-tRNA$^{[Ser]Sec}$ is more detrimental to expression of GPX4 than the lack of SECISBP2. Based on our earlier experiments in *Secisbp2*-deficient mice, we argue that GPX4 maintains a significant level of expression in the absence of SECISBP2 [41,63]. This partial independence from SECISBP2 may significantly contribute to the top position of GPX4 in the hierarchy of selenoproteins, which is further supported by the high affinity of the *GPX4 SECIS* to SECISBP2 [64–70].

As expected from a general selenoprotein deficiency, transcriptomic analyses provided ample evidence for induction of NRF2-regulated genes [13,14], despite some experimental variation among samples. Both brain and heart showed massive induction of NRF2-target genes on postnatal day 1. In adult mice rescued with the *Gpx4*^{Cys} transgene, this gene expression pattern was still evident, but more moderate. In blood and liver, inactivation of both, selenoproteins and NRF2, is incompatible with life [13]. Also in the thyroid, where antioxidative defense is

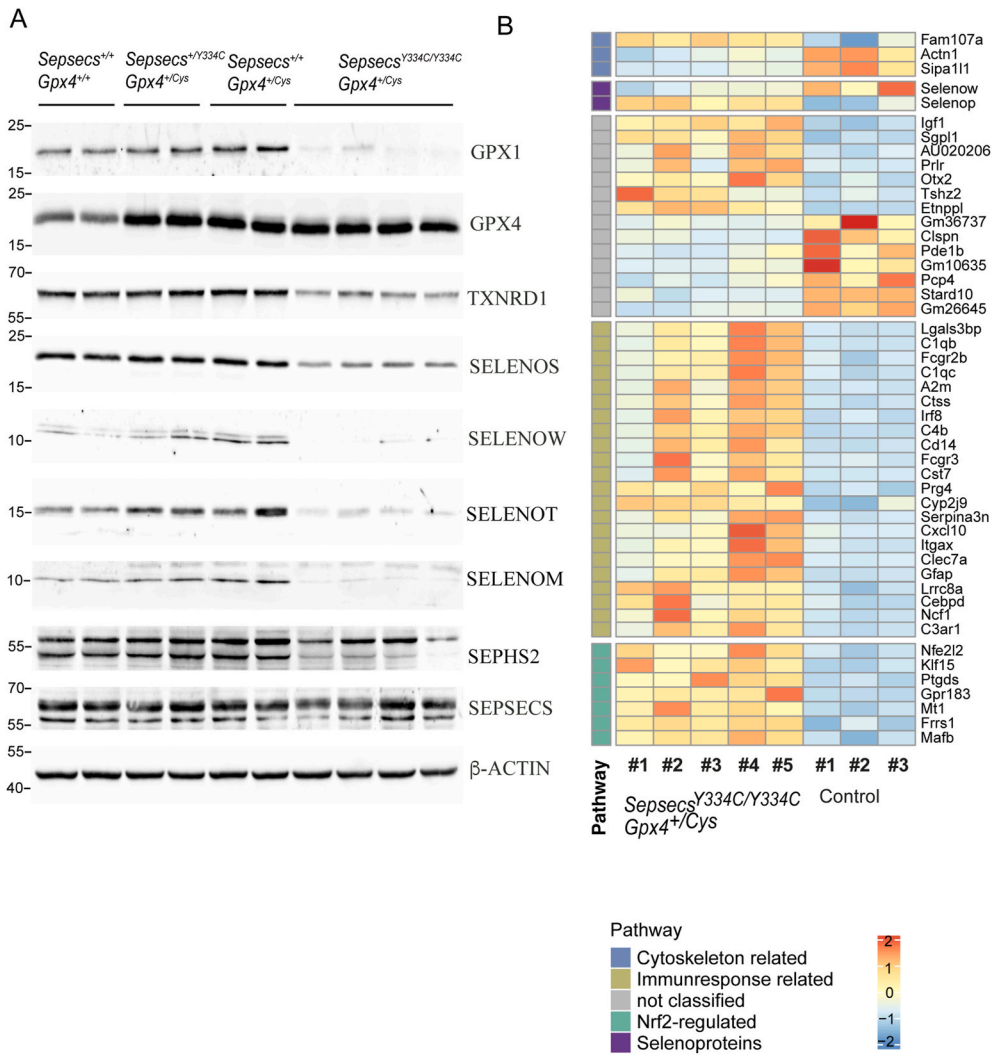

Fig. 10. Cortical gene and selenoprotein expression from *Sepsecs*$^{Y334C/Y334C}$; *Gpx4*$^{+/Cys}$ mice. A) Selenoprotein and SEPSECS expression were detected from cortex of the same animals as in Fig. 9. Beta-actin shows equal loading. B) Up-regulated genes (in red) and downregulated genes (blue) from *Sepsecs*$^{Y334C/Y334C}$; *Gpx4*$^{+/Cys}$ mice (n = 5) and their corresponding controls (n = 3) are represented in a heatmap. Selenoproteins and regulated genes involved in specific pathways or processes are shown. (For interpretation of the references to color in this figure legend, the reader is referred to the Web version of this article.)

thought to be of utmost importance, inactivation of *Trsp* was tolerated possibly because of rescue through NRF2-dependent genes [71–73]. Our results support the notion that among the NRF2-regulated genes is none that can effectively compensate for the loss of GPX4. This explains why GPX4 is essential as a lipid hydroperoxide peroxidase. The ferroptosis modulator FSP1, which can contribute to reduction of lipid hydroperoxides through coenzyme Q [74], was not among the transcriptionally induced genes in any of the samples analyzed by RNA sequencing.

We observed clearly organ-specific responses to SEPSECS-deficiency. For example, pathogenic variants in *SELENOI*/ethanolamine-phosphotransferase 1 have been shown to lead to a neurological disorder in humans [75,76]. The induction of ethanolamine-phospho-lyase (*Etnppl*) and sphingosine-1-phosphate-lyase (*Sgpl1*) in *Sepsecs*$^{Y334C/Y334C}$; *Gpx4*^{Cys} brain and concurrent downregulation of *Stard10* point to an excess of phospho-ethanolamine that results from the impaired expression of SELENOI that normally consumes phospho-ethanolamine for phosphatidyl-ethanolamine biosynthesis (PE). This regulation is only evident in the adult brain transcriptome, but not in the heart, explaining that the role of SELENOI in PE biosynthesis is more important in brain than in heart – compatible with the neurological disorders described [75,76]. Conversely, the dysregulation of cholesterol metabolism is evident in the heart, but not in the brain. Such organ-specific responses, in our eyes, should always be considered when interpreting inborn errors of metabolism.

Several selenoproteins are involved in the maturation of proteins. Accordingly, we find an induction of the UPR and phosphorylation of eIF2a in postnatal and adult heart. Interestingly, UPR is not observed in the brain. Differential penetrance of the *Sepsecs*^{Y334C} variant in different organs adds to this complexity. As evident from the Western blot analyses, kidney and liver were only moderately and not at all affected, respectively, in their capacity to synthesize selenoproteins. We speculate that the expression level of SEPSECS relative to the metabolic requirement of its product may explain this observation. Organ specificity may also be the reason why bone growth is not impaired in the newborn SEPSECS-deficient mice, but in mice with the *Trsp* gene disrupted in cartilage [8]. Interrogating all organ systems regarding their response to the reduction of a given important selenoprotein is clearly beyond the scope of this manuscript.

So why is deficiency of SEPSECS so much more severe than deficiency of SECISBP2? We speculate, based on the data presented here, that deficiency of SEPSECS impairs all selenoproteins, including the essential ones. Among the essential ones, GPX4 has gained a top position in the hierarchy by becoming partially independent of SECISBP2, but it remains sensitive to limitation of Sec-tRNA$^{[Ser]Sec}$.

5. Conclusions

Mice with the homozygous p.Y334C variant in *Sepsecs* resemble patients with Sedaghatian disease more closely than patients carrying the same variant who display pontocerebellar hypoplasia 2D. The evident rescue of perinatal death by expression of a selenium-independent GPX4^{Cys} shows that the most critical selenoprotein in the postnatal

period is GPX4. Other selenoprotein-dependent pathways have apparently the ability to compensate for the lack of other selenoproteins. Hence, patients with a general deficiency in selenoprotein biosynthesis might benefit from any pharmacological intervention that inhibits ferroptotic cell death.

Declaration of competing interest

M.C. is co-founder and shareholder of ROSCUE Therapeutics GmbH. All other authors declare no conflict of interest.

Acknowledgements

The authors acknowledge the help of Dr. Geert Michel, Transgenic Services Charité, Berlin and Dr. Andrè Heimbach, Next Generation Sequencing Core Facility of the Medical Faculty, University of Bonn.

Appendix A. Supplementary data

Supplementary data to this article can be found online at https://doi.org/10.1016/j.redox.2021.102188.

Funding

This work was supported by Universitätsklinikum Bonn and Deutsche Forschungsgemeinschaft (DFG) SCHW914/2-2; SCHW914/5-1 (U. S.). Work in the Conrad lab is supported by funding from DFG CO 291/7-1, CO 291/9-1 and CO 291/10-1, the German Federal Ministry of Education and Research (BMBF), the VIP + program NEUROPROTEKT (03VP04260), the Ministry of Science and Higher Education of the Russian Federation (075-15-2019-1933), and the European Research Council (ERC) under the European Union's Horizon 2020 research and innovation program (grant agreement No. GA 884754).

CoI

M.C. is co-founder and shareholder of ROSCUE Therapeutics GmbH.

References

[1] V.M. Labunskyy, D.L. Hatfield, V.N. Selenoproteins Gladyshev, Molecular pathways and physiological roles, Physiol. Rev. 94 (2014) 739–777.
[2] J. Donovan, P.R. Copeland, Threading the needle: getting selenocysteine into proteins, Antioxidants Redox Signal. 12 (2010) 881–892.
[3] K. Schwarz, C.M. Foltz, Selenium as an integral part of factor 3 against dietary necrotic liver degeneration, Nutrition 15 (1957) 255–264.
[4] B.A. Carlson, R. Tobe, E. Yefremova, P.A. Tsuji, V.J. Hoffmann, U. Schweizer, V. N. Gladyshev, D.L. Hatfield, M. Conrad, Glutathione peroxidase 4 and vitamin e cooperatively prevent hepatocellular degeneration, Redox biology 9 (2016) 22–31.
[5] M. Wortmann, M. Schneider, J. Pircher, J. Hellfritsch, M. Aichler, N. Vegi, P. Kolle, P. Kuhlencordt, A. Walch, U. Pohl, et al., Combined deficiency in glutathione peroxidase 4 and vitamin e causes multiorgan thrombus formation and early death in mice, Circ. Res. 113 (2013) 408–417.
[6] J. Loscalzo, Keshan disease, selenium deficiency, and the selenoproteome, N. Engl. J. Med. 370 (2014) 1756–1760.
[7] E. Varone, D. Pozzer, S. Di Modica, A. Chernorudskiy, L. Nogara, M. Baraldo, M. Cinquanta, S. Fumagalli, R.N. Villar-Quiles, M.G. De Simoni, et al., Selenon (sepn1) protects skeletal muscle from saturated fatty acid-induced er stress and insulin resistance, Redox biology 24 (2019) 101176.
[8] C.M. Downey, C.R. Horton, B.A. Carlson, T.E. Parsons, D.L. Hatfield, B. Hallgrimsson, F.R. Jirik, Osteo-chondroprogenitor-specific deletion of the selenocysteine trna gene, trsp, leads to chondronecrosis and abnormal skeletal development: a putative model for kashin-beck disease, PLoS Genet. 5 (2009), e1000616.
[9] U. Schweizer, S. Bohleber, W. Zhao, N. Fradejas-Villar, The neurobiology of selenium: looking back and to the future, Front. Neurosci. 15 (2021) 652099.
[10] C. Liao, B.A. Carlson, R.F. Paulson, K.S. Prabhu, The intricate role of selenium and selenoproteins in erythropoiesis, Free Radic. Biol. Med. 127 (2018) 165–171.
[11] J. Köhrle, F. Jakob, B. Contempre, J.E. Dumont, Selenium, the thyroid, and the endocrine system, Endocr. Rev. 26 (2005) 944–984.
[12] G.V. Kryukov, S. Castellano, S.V. Novoselov, A.V. Lobanov, O. Zehtab, R. Guigo, V. N. Gladyshev, Characterization of mammalian selenoproteomes, Science 300 (2003) 1439–1443.
[13] T. Suzuki, V.P. Kelly, H. Motohashi, O. Nakajima, S. Takahashi, S. Nishimura, M. Yamamoto, Deletion of the selenocysteine trna gene in macrophages and liver results in compensatory gene induction of cytoprotective enzymes by nrf2, J. Biol. Chem. 283 (2008) 2021–2030.
[14] A. Sengupta, B.A. Carlson, J.A. Weaver, S.V. Novoselov, D.E. Fomenko, V. N. Gladyshev, D.L. Hatfield, A functional link between housekeeping selenoproteins and phase ii enzymes, Biochem. J. 413 (2008) 151–161.
[15] S. Seeher, T. Atassi, Y. Mahdi, B.A. Carlson, D. Braun, E.K. Wirth, M.O. Klein, N. Reix, A.C. Miniard, L. Schomburg, et al., Secisbp2 is essential for embryonic development and enhances selenoprotein expression, Antioxidants Redox Signal. 21 (2014) 835–849.
[16] Y. Saito, Selenium transport mechanism via selenoprotein p-its physiological role and related diseases, Front Nutr 8 (2021) 685517.
[17] S. Verma, F.W. Hoffmann, M. Kumar, Z. Huang, K. Roe, E. Nguyen-Wu, A. S. Hashimoto, P.R. Hoffmann, Selenoprotein k knockout mice exhibit deficient calcium flux in immune cells and impaired immune responses, J. Immunol. 186 (2011) 2127–2137.
[18] A. Sreelatha, S.S. Yee, V.A. Lopez, B.C. Park, L.N. Kinch, S. Pilch, K.A. Servage, J. Zhang, J. Jiou, M. Karasiewicz-Urbanska, et al., Protein ampylation by an evolutionarily conserved pseudokinase, Cell 175 (2018) 809–821, e819.
[19] U. Schweizer, N. Fradejas-Villar, Why 21? The significance of selenoproteins for human health revealed by inborn errors of metabolism, Faseb. J. 30 (2016) 3669–3681.
[20] E. Schoenmakers, M. Agostini, C. Mitchell, N. Schoenmakers, L. Papp, O. Rajanayagam, R. Padidela, L. Ceron-Gutierrez, R. Doffinger, C. Prevosto, et al., Mutations in the selenocysteine insertion sequence-binding protein 2 gene lead to a multisystem selenoprotein deficiency disorder in humans, J. Clin. Invest. 120 (2010) 4220–4235.
[21] A.M. Dumitrescu, X.H. Liao, M.S. Abdullah, J. Lado-Abeal, F.A. Majed, L. C. Moeller, G. Boran, L. Schomburg, R.E. Weiss, S. Refetoff, Mutations in secisbp2 result in abnormal thyroid hormone metabolism, Nat. Genet. 37 (2005) 1247–1252.
[22] O. Agamy, B. Ben Zeev, D. Lev, B. Marcus, D. Fine, D. Su, G. Narkis, R. Ofir, C. Hoffmann, E. Leshinsky-Silver, et al., Mutations disrupting selenocysteine formation cause progressive cerebello-cerebral atrophy, Am. J. Hum. Genet. 87 (2010) 538–544.
[23] A.K. Anttonen, T. Hilander, T. Linnankivi, P. Isohanni, R.L. French, Y. Liu, M. Simonovic, D. Soll, M. Somer, D. Muth-Pawlak, et al., Selenoprotein biosynthesis defect causes progressive encephalopathy with elevated lactate, Neurology 85 (2015) 306–315.
[24] J. Yuan, S. Palioura, J.C. Salazar, D. Su, P. O'Donoghue, M.J. Hohn, A.M. Cardoso, W.B. Whitman, D. Söll, Rna-dependent conversion of phosphoserine forms selenocysteine in eukaryotes and archaea, Proc. Natl. Acad. Sci. U. S. A. 103 (2006) 18923–18927.
[25] X.M. Xu, B.A. Carlson, H. Mix, Y. Zhang, K. Saira, R.S. Glass, M.J. Berry, V. N. Gladyshev, D.L. Hatfield, Biosynthesis of selenocysteine on its trna in eukaryotes, PLoS Biol. 5 (2007) e4.
[26] L.J. Yant, Q. Ran, L. Rao, H. Van Remmen, T. Shibatani, J.G. Belter, L. Motta, A. Richardson, T.A. Prolla, The selenoprotein gpx4 is essential for mouse development and protects from radiation and oxidative damage insults, Free Radic. Biol. Med. 34 (2003) 496–502.
[27] A. Seiler, M. Schneider, H. Forster, S. Roth, E.K. Wirth, C. Culmsee, N. Plesnila, E. Kremmer, O. Radmark, W. Wurst, et al., Glutathione peroxidase 4 senses and translates oxidative stress into 12/15-lipoxygenase dependent- and aif-mediated cell death, Cell Metabol. 8 (2008) 237–248.
[28] M. Conrad, C. Jakupoglu, S.G. Moreno, S. Lippl, A. Banjac, M. Schneider, H. Beck, A.K. Hatzopoulos, U. Just, F. Sinowatz, et al., Essential role for mitochondrial thioredoxin reductase in hematopoiesis, heart development, and heart function, Mol. Cell Biol. 24 (2004) 9414–9423.
[29] C. Jakupoglu, G.K. Przemeck, M. Schneider, S.G. Moreno, N. Mayr, A. K. Hatzopoulos, M.H. de Angelis, W. Wurst, G.W. Bornkamm, M. Brielmeier, et al., Cytoplasmic thioredoxin reductase is essential for embryogenesis but dispensable for cardiac development, Mol. Cell Biol. 25 (2005) 1980–1988.
[30] J.C. Avery, Y. Yamazaki, F.W. Hoffmann, B. Folgelgren, P.R. Hoffmann, Selenoprotein i is essential for murine embryogenesis, Arch. Biochem. Biophys. 689 (2020) 108444.
[31] H. Imai, F. Hirao, T. Sakamoto, K. Sekine, Y. Mizukura, M. Saito, T. Kitamoto, M. Hayasaka, K. Hanaoka, Y. Nakagawa, Early embryonic lethality caused by targeted disruption of the mouse phgpx gene, Biochem. Biophys. Res. Commun. 305 (2003) 278–286.
[32] D. Santesmasses, M. Mariotti, V.N. Gladyshev, Tolerance to selenoprotein loss differs between human and mouse, Mol. Biol. Evol. 37 (2020) 341–354.
[33] L. Boukhzar, A. Hamieh, D. Cartier, Y. Tanguy, I. Alsharif, M. Castex, A. Arabo, S. El Hajji, J.J. Bonnet, M. Errami, et al., Selenoprotein t exerts an essential oxidoreductase activity that protects dopaminergic neurons in mouse models of Parkinson's disease, Antioxid. Redox Signal 24 (11) (2016) 557–574, https://doi.org/10.1089/ars.2015.6478.
[34] A.C. Smith, A.J. Mears, R. Bunker, A. Ahmed, M. MacKenzie, J. A. Schwartzentruber, C.L. Beaulieu, E. Ferretti, F.C. Consortium, J. Majewski, et al., Mutations in the enzyme glutathione peroxidase 4 cause sedaghatian-type spondylometaphyseal dysplasia, J. Med. Genet. 51 (2014) 470–474.
[35] R. Prasad, L.F. Chan, C.R. Hughes, J.P. Kaski, J.C. Kowalczyk, M.O. Savage, C. J. Peters, N. Nathwani, A.J. Clark, H.L. Storr, et al., Thioredoxin reductase 2 (txnrd2) mutation associated with familial glucocorticoid deficiency (fgd), J. Clin. Endocrinol. Metab. 99 (2014) E1556–E1563.

[36] A.P. Kudin, G. Baron, G. Zsurka, K.G. Hampel, C.E. Elger, A. Grote, Y. Weber, H. Lerche, H. Thiele, P. Nurnberg, et al., Homozygous mutation in txnrd1 is associated with genetic generalized epilepsy, Free Radic. Biol. Med. 106 (2017) 270–277.
[37] S. Seeher, B.A. Carlson, A.C. Miniard, E.K. Wirth, Y. Mahdi, D.L. Hatfield, D. M. Driscoll, U. Schweizer, Impaired selenoprotein expression in brain triggers striatal neuronal loss leading to co-ordination defects in mice, Biochem. J. 462 (2014) 67–75.
[38] E. Schoenmakers, K. Chatterjee, Human disorders affecting the selenocysteine incorporation pathway cause systemic selenoprotein deficiency, Antioxidants Redox Signal. 33 (2020) 481–497.
[39] I. Ingold, C. Berndt, S. Schmitt, S. Doll, G. Poschmann, K. Buday, A. Roveri, X. Peng, F. Porto Freitas, T. Seibt, et al., Selenium utilization by gpx4 is required to prevent hydroperoxide-induced ferroptosis, Cell 172 (2018) 409–422 e421.
[40] V.N. Gladyshev, E.S. Arner, M.J. Berry, R. Brigelius-Flohe, E.A. Bruford, R.F. Burk, B.A. Carlson, S. Castellano, L. Chavatte, M. Conrad, et al., Selenoprotein gene nomenclature, J. Biol. Chem. 291 (2016) 24036–24040.
[41] W. Zhao, S. Bohleber, H. Schmidt, S. Seeher, M.T. Howard, D. Braun, S. Arndt, U. Reuter, H. Wende, C. Birchmeier, et al., Ribosome profiling of selenoproteins in vivo reveals consequences of pathogenic secisbp2 missense mutations, J. Biol. Chem. 294 (2019) 14185–14200.
[42] G.M. Beaudoin 3rd, S.H. Lee, D. Singh, Y. Yuan, Y.G. Ng, L.F. Reichardt, J. Arikkath, Culturing pyramidal neurons from the early postnatal mouse hippocampus and cortex, Nat. Protoc. 7 (2012) 1741–1754.
[43] N. Fradejas, C. Serrano-Perez Mdel, P. Tranque, S. Calvo, Selenoprotein s expression in reactive astrocytes following brain injury, Glia 59 (2011) 959–972.
[44] S.H. Brutsch, C.C. Wang, L. Li, H. Stender, N. Neziroglu, C. Richter, H. Kuhn, A. Borchert, Expression of inactive glutathione peroxidase 4 leads to embryonic lethality, and inactivation of the alox15 gene does not rescue such knock-in mice, Antioxidants Redox Signal. 22 (2015) 281–293.
[45] M.R. Sedaghatian, Congenital lethal metaphyseal chondrodysplasia: a newly recognized complex autosomal recessive disorder, Am. J. Med. Genet. 6 (1980) 269–274.
[46] B.N. Chorley, M.R. Campbell, X. Wang, M. Karaca, D. Sambandan, F. Bangura, P. Xue, J. Pi, S.R. Kleeberger, D.A. Bell, Identification of novel nrf2-regulated genes by chip-seq: influence on retinoid x receptor alpha, Nucleic Acids Res. 40 (2012) 7416–7429.
[47] A. Sengupta, B.A. Carlson, V.J. Hoffmann, V.N. Gladyshev, D.L. Hatfield, Loss of housekeeping selenoprotein expression in mouse liver modulates lipoprotein metabolism, Biochem. Biophys. Res. Commun. 365 (2008) 446–452.
[48] S. Dhingra, M.P. Bansal, Attenuation of ldl receptor gene expression by selenium deficiency during hypercholesterolemia, Mol. Cell. Biochem. 282 (2006) 75–82.
[49] E.K. Wirth, M. Conrad, J. Winterer, C. Wozny, B.A. Carlson, S. Roth, D. Schmitz, G. W. Bornkamm, V. Coppola, L. Tessarollo, et al., Neuronal selenoprotein expression is required for interneuron development and prevents seizures and neurodegeneration, Faseb. J. 24 (2010) 844–852.
[50] E.K. Wirth, B.S. Bharathi, D. Hatfield, M. Conrad, M. Brielmeier, U. Schweizer, Cerebellar hypoplasia in mice lacking selenoprotein biosynthesis in neurons, Biol. Trace Elem. Res. 158 (2014) 203–210.
[51] K. Renko, M. Werner, I. Renner-Muller, T.G. Cooper, C.H. Yeung, B. Hollenbach, M. Scharpf, J. Köhrle, L. Schomburg, U. Schweizer, Hepatic selenoprotein p (sepp) expression restores selenium transport and prevents infertility and motor-incoordination in sepp-knockout mice, Biochem. J. 409 (2008) 741–749.
[52] W.M. Valentine, T.W. Abel, K.E. Hill, L.M. Austin, R.F. Burk, Neurodegeneration in mice resulting from loss of functional selenoprotein p or its receptor apolipoprotein e receptor 2, J. Neuropathol. Exp. Neurol. 67 (2008) 68–77.
[53] C.N. Byrns, M.W. Pitts, C.A. Gilman, A.C. Hashimoto, M.J. Berry, Mice lacking selenoprotein p and selenocysteine lyase exhibit severe neurological dysfunction, neurodegeneration, and audiogenic seizures, J. Biol. Chem. 289 (2014) 9662–9674.
[54] M. Kühbacher, J. Bartel, B. Hoppe, D. Alber, G. Bukalis, A.U. Bräuer, D. Behne, A. Kyriakopoulos, The brain selenoproteome: priorities in the hierarchy and different levels of selenium homeostasis in the brain of selenium-deficient rats, J. Neurochem. 110 (2009) 133–142.
[55] S. Palioura, R.L. Sherrer, T.A. Steitz, D. Soll, M. Simonovic, The human sepsecs-trnasec complex reveals the mechanism of selenocysteine formation, Science 325 (2009) 321–325.
[56] A. Fragkouli, N.V. van Wijk, R. Lopes, N. Kessaris, V. Pachnis, Lim homeodomain transcription factor-dependent specification of bipotential mge progenitors into cholinergic and gabaergic striatal interneurons, Development 136 (2009) 3841–3851.
[57] Y. Zhao, O. Marin, E. Hermesz, A. Powell, N. Flames, M. Palkovits, J.L. Rubenstein, H. Westphal, The lim-homeobox gene lhx8 is required for the development of many cholinergic neurons in the mouse forebrain, Proc. Natl. Acad. Sci. U. S. A. 100 (2003) 9005–9010.
[58] A.J. Baucum 2nd, B.C. Shonesy, K.L. Rose, R.J. Colbran, Quantitative proteomics analysis of camkii phosphorylation and the camkii interactome in the mouse forebrain, ACS Chem. Neurosci. 6 (2015) 615–631.
[59] D. Sibbing, A. Pfeufer, T. Perisic, A.M. Mannes, K. Fritz-Wolf, S. Unwin, M. F. Sinner, C. Gieger, C.J. Gloeckner, H.E. Wichmann, et al., Mutations in the mitochondrial thioredoxin reductase gene txnrd2 cause dilated cardiomyopathy, Eur. Heart J. 32 (2011) 1121–1133.
[60] S. Roth, S. Zhang, J. Chiu, E.K. Wirth, U. Schweizer, Development of a serum-free supplement for primary neuron culture reveals the interplay of selenium and vitamin e in neuronal survival, J. Trace Elem. Med. Biol. 24 (2010) 130–137.
[61] J. Zheng, M. Conrad, The metabolic underpinnings of ferroptosis, Cell Metabol. 32 (2020) 920–937.
[62] W.S. Hambright, R.S. Fonseca, L. Chen, R. Na, Q. Ran, Ablation of ferroptosis regulator glutathione peroxidase 4 in forebrain neurons promotes cognitive impairment and neurodegeneration, Redox biology 12 (2017) 8–17.
[63] N. Fradejas-Villar, S. Seeher, C.B. Anderson, M. Doengi, B.A. Carlson, D.L. Hatfield, U. Schweizer, M.T. Howard, The rna-binding protein secisbp2 differentially modulates uga codon reassignment and rna decay, Nucleic Acids Res. 45 (2017) 4094–4107.
[64] G. Bermano, J.R. Arthur, J.E. Hesketh, Role of the 3' untranslated region in the regulation of cytosolic glutathione peroxidase and phospholipid-hydroperoxide glutathione peroxidase gene expression by selenium supply, Biochem. J. 320 (1996) 891–895.
[65] K. Wingler, M. Bocher, L. Flohe, H. Kollmus, R. Brigelius-Flohe, Mrna stability and selenocysteine insertion sequence efficiency rank gastrointestinal glutathione peroxidase high in the hierarchy of selenoproteins, Eur. J. Biochem. 259 (1999) 149–157.
[66] X.G. Lei, J.K. Evenson, K.M. Thompson, R.A. Sunde, Glutathione peroxidase and phospholipid hydroperoxide glutathione peroxidase are differentially regulated in rats by dietary selenium, J. Nutr. 125 (1995) 1438–1446.
[67] J.L. Bubenik, D.M. Driscoll, Altered rna binding activity underlies abnormal thyroid hormone metabolism linked to a mutation in selenocysteine insertion sequence-binding protein 2, J. Biol. Chem. 282 (2007) 34653–34662.
[68] L. Latrèche, O. Jean-Jean, D.M. Driscoll, L. Chavatte, Novel structural determinants in human secis elements modulate the translational recoding of uga as selenocysteine, Nucleic Acids Res. 37 (2009) 5868–5880.
[69] A. Mehta, C.M. Rebsch, S.A. Kinzy, J.E. Fletcher, P.R. Copeland, Efficiency of mammalian selenocysteine incorporation, J. Biol. Chem. 279 (2004) 37852–37859.
[70] J.E. Squires, I. Stoytchev, E.P. Forry, M.J. Berry, Sbp2 binding affinity is a major determinant in differential selenoprotein mrna translation and sensitivity to nonsense-mediated decay, Mol. Cell Biol. 27 (2007) 7848–7855.
[71] J. Chiu-Ugalde, E.K. Wirth, M.O. Klein, R. Sapin, N. Fradejas-Villar, K. Renko, L. Schomburg, J. Kohrle, U. Schweizer, Thyroid function is maintained despite increased oxidative stress in mice lacking selenoprotein biosynthesis in thyroid epithelial cells, Antioxidants Redox Signal. 17 (2012) 902–913.
[72] P.G. Ziros, I.G. Habeos, D.V. Chartoumpekis, E. Ntalampyra, E. Somm, C. O. Renaud, M. Bongiovanni, I.P. Trougakos, M. Yamamoto, T.W. Kensler, et al., Nfe2-related transcription factor 2 coordinates antioxidant defense with thyroglobulin production and iodination in the thyroid gland, Thyroid 28 (2018) 780–798.
[73] C.O. Renaud, P.G. Ziros, D.V. Chartoumpekis, M. Bongiovanni, G.P. Sykiotis, Keap1/nrf2 signaling: a new player in thyroid pathophysiology and thyroid cancer, Front. Endocrinol. 10 (2019) 510.
[74] S. Doll, F.P. Freitas, R. Shah, M. Aldrovandi, M.C. da Silva, I. Ingold, A. Goya Grocin, T.N. Xavier da Silva, E. Panzilius, C.H. Scheel, et al., Fsp1 is a glutathione-independent ferroptosis suppressor, Nature 575 (2019) 693–698.
[75] M.Y. Ahmed, A. Al-Khayat, F. Al-Murshedi, A. Al-Futaisi, B.A. Chioza, J. Pedro Fernandez-Murray, J.E. Self, C.G. Salter, G.V. Harlalka, L.E. Rawlins, et al., A mutation of ept1 (selenoi) underlies a new disorder of kennedy pathway phospholipid biosynthesis, Brain 140 (2017) 547–554.
[76] Y. Horibata, O. Elpeleg, A. Eran, Y. Hirabayashi, D. Savitzki, G. Tal, H. Mandel, H. Sugimoto, Ept1 (selenoprotein i) is critical for the neural development and maintenance of plasmalogen in humans, J. Lipid Res. 59 (2018) 1015–1026.